

FETI-DP FOR THE THREE-DIMENSIONAL VIRTUAL ELEMENT METHOD

SILVIA BERTOLUZZA, MICOL PENNACCHIO, AND DANIELE PRADA

ABSTRACT. We deal with the Finite Element Tearing and Interconnecting Dual Primal (FETI-DP) preconditioner for elliptic problems discretized by the virtual element method (VEM). We extend the result of [16] to the three dimensional case. We prove polylogarithmic condition number bounds, independent of the number of subdomains, the mesh size, and jumps in the diffusion coefficients. Numerical experiments validate the theory.

1. INTRODUCTION

Methods for the solution of PDEs based on polytopal meshes have recently attracted an increasing attention, mainly due to the necessity of tackling what is nowadays a bottleneck in the overall process of simulating real life phenomena, namely the task of mesh generation. Several methods have been recently introduced which allow for quite general polygonal or polyhedral elements, such as Mimetic Finite Differences [11, 19], Discontinuous Galerkin-Finite Element Method (DG-FEM) [1, 22], Hybridizable and Hybrid High-Order Methods [24, 26], Weak Galerkin Method [47], BEM-based FEM [42] and Polygonal FEM [44] to name a few.

Here we deal with the Virtual Element Method (VEM) [5], a discretization technique which can be considered as an extension of the Finite Element Method to polytopal tessellations. In such a method, local approximation spaces containing polynomial functions are defined and assembled in a global conforming approximation space, but the explicit construction and integration of the associated shape functions is avoided, whence the name *virtual* [5]. The evaluation of the operators and matrices needed in the implementation of the method are carried out by only relying on an implicit knowledge of the local shape functions, as described in [7] (see also [4, 10, 37], where the p and hp versions of the method are discussed and analyzed). Though introduced fairly recently, such a method has already been applied and extended to a wide variety of different model problems; we recall applications to: parabolic problems [46], Cahn-Hilliard, Stokes, Navier-Stokes and Helmholtz equations [2, 3, 12, 13, 40], linear and nonlinear elasticity problems [25, 6, 29], general elliptic problems in mixed form [8], fracture networks [14], Laplace-Beltrami equation [28].

In this paper we focus on the linear system of equations associated with the VEM discretization. As it happens in the case of finite element, the efficient solution of such a linear system is of paramount importance to fully exploit the potential of the method. Little work has been done on this issue up to now, all limited to the spatial dimension two. First works in the literature tackled the increase of the condition number appearing already at the level of the elementary stiffness matrix, due either to a degradation of the quality of the tessellation and/or to the increase in the polynomial order of the method [10, 36, 15]. If we rather consider the increase of the condition number resulting from refining the discretization, to the best of our knowledge the approaches considered up to now are domain decomposition ([21, 20, 16, 41]) and multigrid ([4], for p refinement). In the present paper we extend to the three dimensional case the results obtained in [16]. More precisely, we focus on one of the most efficient preconditioning techniques: the Dual-Primal Finite Element Tearing

Date: December 4, 2018.

This paper has been realized in the framework of ERC Project CHANGE, which has received funding from the European Research Council (ERC) under the European Unions Horizon 2020 research and innovation programme (grant agreement No 694515).

and Interconnecting (FETI-DP) [27], [45], a non overlapping domain decomposition method where the problem is reformulated as a constrained optimization problem and solved by iterating on the set of Lagrange multipliers representing the fluxes across the interface between the non overlapping subdomains. The FETI-DP method has been already extensively studied in the context of many different discretization methods – spectral elements [38, 31], mortar discretizations [30], NURBS discretizations in isogeometric analysis [39].

Following the approach presented in [16] for two dimensional domains, we prove that the properties of scalability, quasi-optimality and independence on the discontinuities of the elliptic operator coefficients across subdomain interfaces, that are known for the finite element case, still hold when dealing with VEM. More specifically, we show that the condition number of the preconditioned matrix is bounded by a constant times the factor $(1 + \log(H/h))^2$, where H and h are, respectively, mesh-size of the subdomain decomposition and of the tessellation, see Theorem 4.7. In order to do so, we need to prove several inequalities related to the VEM approximation space, by only relying on the implicit definition of the discrete functions, which, we recall, are not explicitly known.

We observe that, since we are in the framework of [35], the equivalence of the BDDC (Balancing Domain Decomposition by Constraint) and the FETI-DP preconditioners holds. Therefore the bound for the condition number here obtained also yields an estimate on the BDDC preconditioner for VEM.

The paper is organized as follows. The basic notation, functional setting and the description of the Virtual Element Method are given in Section 2. The dual-primal preconditioner is introduced and analyzed in Section 4, whereas some relevant properties of the VE discretization space mainly used for the proof are presented in Section 3. The analysis of the preconditioner, with the proof of the estimate for the condition number (Theorem 4.7), is carried out in section 5 where we also give some detail specific to its implementation in the VEM framework. Numerical experiments that validate the theory are presented in Section 6.

2. THE VIRTUAL ELEMENT METHOD (VEM)

Notations. As we are interested here in explicitly studying the dependence of the estimates that we are going to prove on the number and size of the subdomains and the number and size of the elements of the tessellations, throughout the paper we will employ the notation $A \lesssim B$ (resp. $A \gtrsim B$) to say that the quantity A is bounded from above (resp. from below) by cB , with a constant c independent of the diffusion coefficient ρ in the PDE (and in particular, independent of M , α and of its jump across the interface of the decomposition), and depending on the tessellation and on the decomposition only via the (possibly implicit) constants in Assumptions 2.2 and 4.1. The expression $A \simeq B$ will stand for $A \lesssim B \lesssim A$.

The Virtual Element Discretization. We start by recalling the definition and the main properties of the Virtual Element Method [5] and, to fix the ideas, we focus on the following elliptic model problem:

$$-\nabla \cdot (\rho \nabla u) = g \quad \text{in } \Omega, \quad u = 0 \quad \text{on } \partial\Omega,$$

with $g \in L^2(\Omega)$, where $\Omega \subset \mathbb{R}^3$ is (for simplicity) a convex polyhedron. We assume that the coefficient ρ is a scalar such that for almost all $x \in \Omega$, $\alpha \leq \rho(x) \leq M$ for two constants $M \geq \alpha > 0$. The variational formulation of such an equation reads

$$(2.1) \quad \begin{cases} \text{find } u \in V := H_0^1(\Omega) \text{ such that} \\ a(u, v) = (f, v) \quad \forall v \in V \end{cases}$$

with

$$a(u, v) = \int_{\Omega} \rho(x) \nabla u(x) \cdot \nabla v(x) \, dx, \quad (g, v) = \int_{\Omega} g(x) v(x) \, dx.$$

We consider a family $\{\mathcal{T}_h\}_h$ of tessellations of Ω into a finite number of polyhedra K .

Definition 2.1. We say that a polyhedron K is shape regular of diameter h if there exist $\gamma_K > 0$ such that K satisfies the following assumptions ([33]):

- (1) for every element K , every face f and every edge e we have

$$\gamma_K h^3 \leq |K|, \quad \gamma_K h^2 \leq |f|, \quad \gamma_K h \leq |e|.$$

- (2) for each face f , there exists a point $\mathbf{x}_f \in f$ such that f is star-shaped with respect to every point in the disk of radius $\gamma_K h$ centered at \mathbf{x}_f ;
(3) for each element K , there exists a point \mathbf{x}_K such that K is star-shaped with respect to every point in the sphere of radius $\gamma_K h$ centered at \mathbf{x}_K .
(4) for every element K , and for every face f of K , there exists a pyramid contained in K such that its base equals to f , its height equals to $\gamma_K h$ and the projection of its vertex onto f is \mathbf{x}_f .

Assumption 2.2. We assume that there exist two constants N_\star and γ_\star such that the tessellation \mathcal{T}_h verifies the following assumptions

- (1) \mathcal{T}_h is geometrically conforming, that is for each K, K' in \mathcal{T}_h , $\bar{K} \cap \bar{K}'$ is either the empty set, a vertex, an edge or a face of both K and K' ;
(2) every element K has at most N_\star faces and each face has at most N_\star edges.
(3) all $K \in \mathcal{T}_h$ are shape regular of diameter h_K with $\gamma_K \geq \gamma_\star$;
(4) the tessellation is quasi uniform, that is there exists an h such that for all $K \in \mathcal{T}_h$ $h_K \simeq h$.

The lowest order Virtual Element discretization space is defined element by element starting from the edges of the tessellation, where the discrete functions are defined as linear. On the boundary of each face f we then introduce the space:

$$\mathbb{B}_1(\partial f) = \{g \in C^0(\partial f) : g|_e \in \mathbb{P}_1(e) \text{ for all edge } e \subseteq f\}$$

where, for any one, two or three dimensional domain D , $\mathbb{P}_1(D)$ denotes the set of order 1 polynomials on D . On each face f we then define the space $V^{f,1}$ of local discrete functions as follows

$$(2.2) \quad V^{f,1} = \{v \in C^0(f) : v|_{\partial f} \in \mathbb{B}_1(\partial f), \Delta v \in \mathbb{P}_1(f) \text{ and } \int_f qv = \int_f q \Pi_f^\nabla v, \forall q \in \mathbb{P}_1(f)\},$$

where $\Pi_f^\nabla : C^0(f) \rightarrow \mathbb{P}_1(f)$ denotes the projection onto the space of order one polynomials, orthogonal with respect to the scalar product

$$(2.3) \quad (v, w)_{1,f} = \int_f \nabla v(x) \cdot \nabla w(x) + \left(\sum_{V \text{ vertex of } f} v(V) \right) \left(\sum_{V \text{ vertex of } f} w(V) \right).$$

Observe that the values at the vertices of f uniquely determine the (piecewise linear) trace of any function v in $V^{f,1}$ on ∂f , which, in turn, uniquely determines (and allows to compute) $\Pi_f^\nabla v$. Indeed, for $q \in \mathbb{P}_1(K)$, Green's formula yields

$$(2.4) \quad \int_f \nabla v(x) \cdot \nabla q(x) dx = \int_{\partial f} v(s) \nabla q(s) \cdot \mathbf{n}_f(s) ds.$$

As a function in $H^1(f)$ with linear Laplacian is uniquely defined by its trace on ∂f and by its moments up to order one (which, by definition, for $v \in V^{f,1}$ coincide with those of $\Pi_f^\nabla v$), the values of any function $v \in V^{f,1}$ at the vertices of f uniquely determine v .

We can then assemble the local face spaces to build local spaces on the boundary of K :

$$\mathbb{B}_1(\partial K) := \left\{ g \in C^0(\partial K) : g|_f \in V^{f,1} \text{ for all face } f \subseteq \partial K \right\}$$

and on K

$$(2.5) \quad V^{K,1} := \{v \in H^1(K) : v|_{\partial K} \in \mathbb{B}_1(\partial K) \text{ and } v \text{ harmonic in } K\}.$$

Finally we define:

$$V_h := \{V \in H_0^1(\Omega) : v|_K \in V^{K,1} \text{ for all } K \in \mathcal{T}_h\}.$$

It is not difficult to check that a function in $V^{K,1}$ is uniquely determined by its values at the vertices of K , and consequently, that all functions in V_h are uniquely determined by their values at the vertices of the tessellation. However, they are not known in closed form, so that it is not possible to directly evaluate the bilinear form a on two of such functions (this would imply solving a Poisson equation in each element). The Virtual Element Method is constructed by replacing the bilinear form a with a suitable approximation. This can be achieved starting from the observation that given any $v \in V^{K,1}$ and any $w \in \mathbb{P}_1(K)$ we can easily compute $a^K(u, v)$ by using Green's formula (we are assuming, for the sake of simplicity, that ρ is piecewise constant on the elements of the tessellation, that is, $\rho|_K = \rho_K$)

$$a^K(v, w) = -\rho_K \int_K v \Delta w + \rho_K \int_{\partial K} v \frac{\partial w}{\partial n} = \rho_K \int_{\partial K} v \frac{\partial w}{\partial n}.$$

The right hand side can in fact be computed exactly since on each edge of K $\partial w/\partial n$ is a known constant, and, in view of the the definition of $V^{K,1}$, it is possible to compute the integral of v against such a constant in terms of the degrees of freedom. It is then possible to evaluate, for each $v \in V^{K,1}$, its projection $\Pi_K^\nabla : V^{K,1} \rightarrow \mathbb{P}_1(K)$, onto the space of linears, orthogonal with respect to the scalar product (2.3). Clearly we have

$$(2.6) \quad a^K(u, v) = a^K(\Pi_K^\nabla u, \Pi_K^\nabla v) + a^K(u - \Pi_K^\nabla u, v - \Pi_K^\nabla v).$$

The virtual element method stems from replacing the second term on the right hand side, which cannot be computed exactly, with an “equivalent” operator S_a^K . We then define

$$a_h^K(u, v) = a^K(\Pi_K^\nabla u, \Pi_K^\nabla v) + S_a^K(u - \Pi_K^\nabla u, v - \Pi_K^\nabla v),$$

where S_a^K is any continuous symmetric bilinear form satisfying

$$(2.7) \quad a^K(v, v) \simeq S_a^K(v, v) \quad \forall v \in V^{K,1} \quad \text{with } \Pi_K^\nabla v = 0.$$

Equations (2.6) and (2.7) immediately yield

$$(2.8) \quad a^K(v, v) \simeq a_h^K(v, v) \quad \forall v \in V^{K,1} \quad \text{and} \quad a^K(v, w) = a_h^K(v, w) \text{ whenever } v \text{ or } w \in \mathbb{P}_1(K).$$

Finally, we let $a_h : V_h \times V_h \rightarrow \mathbb{R}$ be defined by

$$a_h(u_h, v_h) = \sum_K a_h^K(u_h, v_h),$$

and we consider the following discrete problem:

Problem 2.3. Find $u_h \in V_h$ such that

$$a_h(u_h, v_h) = \int_\Omega g v_h \quad \forall v_h \in V_h.$$

For the study of the convergence, stability and robustness properties of the method we refer to [5, 9]

3. SOME RELEVANT PROPERTIES OF THE VE DISCRETIZATION SPACE

In this section we present some bounds that will play a role in the forthcoming analysis. More precisely, letting $K \subseteq \mathbb{R}^3$ be a shape regular polyhedron of diameter h , and letting f be any face of K , we have the following bounds.

Agmon inequality. For all functions in $H^1(f)$, it holds [33]

$$(3.1) \quad \int_{\partial f} |u|^2 \lesssim h^{-1} \int_f |u|^2 + h \int_f |\nabla u|^2.$$

Inverse estimates. The following two inverse inequality hold for all $v_h \in V^{f,1}$ [23]:

$$(3.2) \quad \int_f |\Delta v_h|^2 \lesssim h^{-2} \int_f |\nabla v_h|^2,$$

$$(3.3) \quad \int_f |\nabla v_h|^2 \lesssim h^{-2} \int_f |v_h|^2.$$

Riesz basis property. We have the following Lemma.

Lemma 3.1. *Let K be a shape regular polyhedron in three dimensions, let f be a face of K , with vertices V_1, \dots, V_N , and let $v_h \in V^{f,1}$. Then*

$$(3.4) \quad \int_f |v_h|^2 \simeq h^2 \sum_{i=1}^N |v_h(V_i)|^2.$$

Proof. Let us at first prove that the left hand side of (3.4) is less or equal than a constant times the right hand side. We start by observing that

$$\int_f |\hat{v}_h|^2 \lesssim h^2 \sum_i |\hat{v}_h(V_i)|^2,$$

where \hat{v}_h is the solution to

$$-\Delta \hat{v}_h = 0 \text{ in } f, \quad \hat{v}_h = v_h \text{ on } \partial f.$$

In fact, using the maximum principle, since \hat{v}_h is harmonic on the faces, $|f| \lesssim h^2$, and f has at most N_\star vertices, we have

$$(3.5) \quad \int_f |\hat{v}_h|^2 \lesssim h^2 \max_f |\hat{v}_h(x)|^2 \lesssim h^2 \max_{\partial f} |v_h|^2 \lesssim h^2 \max_i |v_h(V_i)|^2 \lesssim h^2 \sum_i |v_h(V_i)|^2.$$

Now we can write

$$(3.6) \quad \int_f |v_h|^2 \lesssim \int_f |\hat{v}_h|^2 + \int_f |v_h - \hat{v}_h|^2.$$

It is not difficult to check that, as $v_h = \hat{v}_h$ on ∂f , it holds that $\Pi_f^\nabla v_h = \Pi_f^\nabla \hat{v}_h$. Thus, integrating by part and using the definition of $V^{f,1}$, we can write (as $\Delta(v_h - \hat{v}_h) \in \mathbb{P}_1(f)$)

$$\int_f |\nabla(v_h - \hat{v}_h)|^2 = - \int_f (v_h - \hat{v}_h) \Delta(v_h - \hat{v}_h) = - \int_f (\Pi_f^\nabla \hat{v}_h - \hat{v}_h) \Delta(v_h - \hat{v}_h),$$

since, from (2.2), for all $v_h \in V^{f,1}$ and all $q \in \mathbb{P}_1(f)$ it holds

$$\int_f v_h q = \int_f \Pi_f^\nabla v_h q.$$

Then

$$(3.7) \quad \int_f |\nabla(v_h - \widehat{v}_h)|^2 \leq \left(\int_f |\Pi_f^\nabla \widehat{v}_h - \widehat{v}_h|^2 \right)^{1/2} \left(\int_f |\Delta(v_h - \widehat{v}_h)|^2 \right)^{1/2} \\ \lesssim \left(\int_f |\nabla \widehat{v}_h|^2 \right)^{1/2} \left(\int_f |\nabla(v_h - \widehat{v}_h)|^2 \right)^{1/2},$$

where we used a direct inequality for the first term (Π_f^∇ is a bounded operator that preserves linears), and an inverse inequality for the second. Dividing both sides by the second factor in the product on the right hand side we obtain

$$\left(\int_f |\nabla(v_h - \widehat{v}_h)|^2 \right)^{1/2} \lesssim \left(\int_f |\nabla \widehat{v}_h|^2 \right)^{1/2}.$$

Then, using Poincaré inequality, we can write

$$(3.8) \quad \int_f |v_h - \widehat{v}_h|^2 \lesssim h^2 \int_f |\nabla(v_h - \widehat{v}_h)|^2 \lesssim h^2 \int_f |\nabla \widehat{v}_h|^2 \lesssim \int_f |\widehat{v}_h|^2,$$

where the last bound is obtained by using once again an inverse inequality. Hence collecting (3.6), (3.5) and (3.8), we get

$$\int_f |v_h|^2 \lesssim h^2 \sum_i |v_h(V_i)|^2.$$

Let us prove the converse inequality. We have

$$h^2 \sum_i |v_h(V_i)|^2 \lesssim h \|v_h\|_{0,\partial f}^2 \lesssim \int_f |v_h|^2 + h^2 |v_h|_{1,f}^2 \lesssim \int_f |v_h|^2,$$

where we used (3.1) and (3.3). \square

4. DOMAIN DECOMPOSITION FOR THE VIRTUAL ELEMENT METHOD

4.1. The subdomain decomposition. We assume that \mathcal{T}_h can be split as $\mathcal{T}_h = \cup_\ell \mathcal{T}_h^\ell$, inducing a decomposition of Ω as the union of L disjoint polyhedral subdomains Ω^ℓ

$$(4.1) \quad \bar{\Omega} = \cup_\ell \bar{\Omega}^\ell \quad \text{with} \quad \bar{\Omega}^\ell = \cup_{K \in \mathcal{T}_h^\ell} K.$$

We will refer to the edges and faces of the Ω^ℓ 's as macro edges and macro faces. We let $\Gamma = \cup \partial \Omega^\ell \setminus \partial \Omega$ denote the skeleton of the decomposition, \mathcal{E}_H and \mathcal{F}_H denote respectively the set of macro-edges E and of macro-faces F of the subdomain decomposition interior to Ω , and \mathcal{F}_H^ℓ and \mathcal{E}_H^ℓ denote the set of, respectively, macro faces and macro edges of the subdomain Ω^ℓ .

Assumption 4.1. We make the following assumptions:

- (1) the subdomain decomposition is geometrically conforming, that is, for each ℓ, m , $\partial \Omega^\ell \cap \partial \Omega^m$ is either a vertex or a whole edge or a whole face of both Ω^ℓ and Ω^m ;
- (2) the subdomains Ω^ℓ are shape regular (in the sense of Definition 2.1) of diameter H_ℓ .
- (3) for all ℓ , there exists a scalar $\rho_\ell > 0$ such that $\rho|_{\Omega^\ell} \simeq \rho_\ell$.
- (4) the decomposition is quasi uniform: there exists an H such that for all ℓ we have $H_\ell \simeq H$.

Remark 4.2. We would like to point out that Assumption 4.1 is actually also an assumption on the tessellation \mathcal{T}_h , satisfied, for instance, if \mathcal{T}_h is built by first introducing the Ω^ℓ 's and then refining them.

Notation: global vs local degrees of freedom. In the following we will need to single out subsets of nodes and edges. To this end, letting Υ denote the set of vertices of \mathcal{T}_h ,

$$\Upsilon = \{y_i, i = 1, \dots, N\} = \text{set of nodes of } \mathcal{T}_h,$$

we let

$$\mathcal{Y} = \{i : y_i \in \Gamma\} = \text{set of (pointers to the) nodes on } \Gamma.$$

For each subdomain Ω^ℓ we let $\mathcal{Y}^\ell \subset \mathcal{Y}$

$$\mathcal{Y}^\ell = \{i : y_i \in \partial\Omega^\ell\}$$

denote the set of indices pointing to nodes on the boundary of Ω^ℓ . We let \mathcal{X} and \mathcal{X}^ℓ denote, respectively, the set of indices of cross-points (vertices of the subdomain decomposition) and of the vertices of the subdomain Ω^ℓ

$$\mathcal{X} = \{i : y_i \text{ is a cross point}\}, \quad \mathcal{X}^\ell = \mathcal{X} \cap \mathcal{Y}^\ell.$$

Finally we let \mathcal{W} be the set of indices of nodes on the wire basket, i.e. on the union of edges of the decomposition.

For each macroedge E and for each macroface F we let

$$\mathcal{Y}_E = \{i : y_i \in \bar{E}\}, \quad \mathcal{Y}_F = \{i : y_i \in \bar{F}\}$$

denote the set of indices of nodes belonging to E and F respectively and

$$\mathcal{W}^\ell = \mathcal{W} \cap \mathcal{Y}^\ell, \quad \mathcal{W}_F = \mathcal{W} \cap \mathcal{Y}_F = \{i : y_i \in \partial F\}.$$

For each node y_i on the skeleton of the decomposition we let \mathcal{N}_i denote the set of the indices of those subdomains whose boundary y_i belongs to:

$$\mathcal{N}_i = \{\ell : y_i \in \partial\Omega^\ell\}, \quad n_i = \#(\mathcal{N}_i).$$

For each edge $E \in \mathcal{E}_H$ and face $f \in \mathcal{F}_H$ we can also define the set \mathcal{N}_E and \mathcal{N}_F of the indices of those subdomains that share, respectively, E and F as an edge or face:

$$\mathcal{N}_E = \{\ell : E \subset \partial\Omega^\ell\}, \quad \mathcal{N}_F = \{\ell : F \subset \partial\Omega^\ell\}.$$

Remark that for all $i \in \mathcal{Y}_E \setminus \mathcal{X}$ we have $\mathcal{N}_i = \mathcal{N}_E$.

Notation: Scaled norms and seminorms. In the following we will make use of suitably scaled norms for the Sobolev spaces defined on faces and edges of the subdomains. More precisely, letting $\hat{\Omega}$ and $\hat{\Gamma}$ denote any three-dimensional and two-dimensional domain with diameter \hat{H} we set:

$$(4.2) \quad \|w\|_{L^2(\hat{\Omega})}^2 = \hat{H}^{-2} \int_{\hat{\Omega}} |w(x)|^2 dx, \quad \|w\|_{L^2(\hat{\Gamma})}^2 = \hat{H}^{-1} \int_{\hat{\Gamma}} |w(\tau)|^2 d\tau,$$

$$(4.3) \quad |w|_{H^1(\hat{\Omega})}^2 = \int_{\hat{\Omega}} |\nabla w(x)|^2 dx, \quad |w(\tau)|_{H^1(\hat{\Gamma})}^2 = \hat{H} \int_{\hat{\Gamma}} |w'(\tau)|^2 d\tau,$$

$$(4.4) \quad |w|_{H^s(\hat{\Gamma})}^2 = \hat{H}^{2s-1} \int_{\hat{\Gamma}} d\sigma \int_{\hat{\Gamma}} d\tau \frac{|w(\sigma) - w(\tau)|^2}{|\sigma - \tau|^{2s+1}}, \quad 0 < s < 1,$$

$$(4.5) \quad \|w\|_{H^1(\hat{\Omega})}^2 = \|w\|_{L^2(\hat{\Omega})}^2 + |w|_{H^1(\hat{\Omega})}^2, \quad \|w\|_{H^s(\hat{\Gamma})}^2 = \|w\|_{L^2(\hat{\Gamma})}^2 + |w|_{H^s(\hat{\Gamma})}^2, \quad 0 < s \leq 1.$$

Domain decomposition and FETI-DP preconditioner. The subdomain spaces V_h^ℓ and bilinear forms $a_h^\ell : V_h^\ell \times V_h^\ell \rightarrow \mathbb{R}$ are defined, as usual, as

$$V_h^\ell = V_h|_{\Omega^\ell}, \quad a_h^\ell(u_h, v_h) = \sum_{K \in \mathcal{T}_h^\ell} a_h^K(u_h, v_h).$$

In view of (2.8) we immediately obtain that for all $u_h, v_h \in V_h^\ell$

$$a_h^\ell(u_h, v_h) \lesssim |u_h|_{1, \Omega^\ell} |v_h|_{1, \Omega^\ell}, \quad a_h^\ell(u_h, u_h) \simeq |u_h|_{1, \Omega^\ell}^2.$$

Solving Problem 2.3 is then reduced to finding $u_h = (u_h^\ell)_\ell \in \prod V_h^\ell$ minimizing

$$J(u_h) = \frac{1}{2} \sum_\ell a_h^\ell(u_h^\ell, u_h^\ell) - \int_\Omega g u_h$$

subject to a continuity constraint across the interface.

The FETI-DP preconditioner is then constructed according to the same strategy used in the finite element case, which we recall, mainly to fix some notation. We let

$$\mathring{V}_h = \prod \mathring{V}_h^\ell, \quad \text{with} \quad \mathring{V}_h^\ell = V_h^\ell \cap H_0^1(\Omega^\ell),$$

and

$$(4.6) \quad W_h = \prod_\ell W_h^\ell, \quad \text{with} \quad W_h^\ell = V_h^\ell|_{\partial\Omega^\ell}.$$

Moreover, for each macro face F and macro edge E we let

$$W_h^F = V_h|_F \quad \text{and} \quad W_h^E = V_h|_E$$

denote, respectively, the trace on F and E of V_h . On W_h we define a norm and a seminorm:

$$\|w_h\|_{1/2,*}^2 = \sum_\ell \rho^\ell \|w_h^\ell\|_{H^{1/2}(\partial\Omega^\ell)}^2, \quad |w_h|_{1/2,*}^2 = \sum_\ell \rho^\ell |w_h^\ell|_{H^{1/2}(\partial\Omega^\ell)}^2.$$

As usual, we define local discrete harmonic lifting operators $\mathcal{L}_h^\ell : W_h^\ell \rightarrow V_h^\ell$ as

$$(4.7) \quad a_h^\ell(\mathcal{L}_h^\ell w_h, v_h) = 0 \quad \forall v_h \in \mathring{V}_h^\ell, \quad \mathcal{L}_h^\ell w_h = w_h \quad \text{on} \quad \partial\Omega^\ell.$$

The following proposition holds

Proposition 4.3. \mathcal{L}_h^ℓ is well defined, and it verifies

$$|\mathcal{L}_h^\ell w_h|_{H^1(\Omega^\ell)} \simeq |w_h|_{H^{1/2}(\partial\Omega^\ell)}.$$

Proof. We start by recalling that there exists a linear operator $\Pi_{SZ} : H^1(\Omega^\ell) \rightarrow V_h^\ell$ such that, for $v \in H^{1+s}$, $0 \leq s \leq 1$ one has ([23])

$$(4.8) \quad \|v - \Pi_{SZ} v\|_{L^2(\Omega^\ell)} + \frac{h}{H} |v - \Pi_{SZ} v|_{H^1(\Omega^\ell)} \lesssim \left(\frac{h}{H}\right)^{1+s} |v|_{H^{1+s}(\Omega^\ell)},$$

(note that we are using scaled norms, see (4.2–4.5)). Moreover Π_{SZ} is constructed in such a way that if $v|_{\partial\Omega^\ell} \in W_h^\ell$ one has $\Pi_{SZ} v = v$ on $\partial\Omega^\ell$. In view of this result it is not difficult to construct an operator $L_h^\ell : W_h^\ell \rightarrow V_h^\ell$ satisfying $L_h^\ell w_h|_{\partial\Omega^\ell} = w_h$ and

$$(4.9) \quad |L_h^\ell w_h|_{H^1(\Omega^\ell)} \leq |w_h|_{H^{1/2}(\partial\Omega^\ell)}.$$

L_h^ℓ can be for instance defined as Π_{SZ} applied to the harmonic lifting of w_h ; (4.9) follows then from the stability of the harmonic lifting and of Π_{SZ} , exactly as in the two dimensional case [16]. We can then write

$$\begin{aligned} |\mathcal{L}_h^\ell w_h - L_h^\ell w_h|_{H^1(\partial\Omega^\ell)}^2 &\lesssim a_h^\ell(\mathcal{L}_h^\ell w_h - L_h^\ell w_h, \mathcal{L}_h^\ell w_h - L_h^\ell w_h) \\ &= -a_h^\ell(L_h^\ell w_h, \mathcal{L}_h^\ell w_h - L_h^\ell w_h) \lesssim |L_h^\ell w_h|_{H^1(\partial\Omega^\ell)} |\mathcal{L}_h^\ell w_h - L_h^\ell w_h|_{H^1(\partial\Omega^\ell)}. \end{aligned}$$

In view of (4.9) it is easy to conclude by applying a triangular inequality. \square

Let now $\widehat{W}_h \subset W_h$ denote the subset of functions which are single valued across Γ :

$$(4.10) \quad \begin{aligned} \widehat{W}_h &= \{w_h \in W_h : \forall x \in \bar{\Omega}^\ell \cap \bar{\Omega}^k, w_h^\ell(x) = w_h^k(x)\} \\ &= \{w_h \in W_h : \forall i \in \mathcal{Y}, \ell, m \in \mathcal{N}_i \Rightarrow w_h^\ell(y_i) = w_h^m(y_i)\}. \end{aligned}$$

For $w_h = (w_h^\ell)_\ell \in W_h$ we let $\mathcal{L}_h(w_h) = (\mathcal{L}_h^\ell w_h^\ell)_\ell$, so that V_h is split as

$$(4.11) \quad V_h = \mathring{V}_h \oplus \mathcal{L}_h \widehat{W}_h.$$

We next define the bilinear for $s : W_h \times W_h \rightarrow \mathbb{R}$ as

$$s(w_h, v_h) := \sum_\ell a_h^\ell(\mathcal{L}_h^\ell w_h, \mathcal{L}_h^\ell v_h).$$

The proof of the following proposition is trivial.

Proposition 4.4. *For all $v_h, w_h \in W_h$ we have*

$$(4.12) \quad s(v_h, w_h) \lesssim |w_h|_{1/2,*} |v_h|_{1/2,*}, \quad s(w_h, w_h) \gtrsim |w_h|_{1/2,*}^2.$$

Problem 2.3 is then split as the combination of two independent problems

Problem 4.5. Find $\mathring{u}_h \in \mathring{V}_h$ such that for all $v_h \in \mathring{V}_h$

$$a_h(\mathring{u}_h, v_h) = \int_\Omega g v_h.$$

Problem 4.6. Find $w_h \in \widehat{W}_h$ such that for all $v_h \in \widehat{W}_h$

$$s(w_h, v_h) = \int_\Omega g \mathcal{L}_h v_h.$$

Exactly as in the finite element case, the design of different versions of the FETI-DP method will rely on the choice of a subspace \widetilde{W}_h of W_h whose elements have some degree of continuity on Γ , ensuring that the restriction to \widetilde{W}_h of the bilinear form a_h is coercive (which is equivalent to asking that the seminorm $|\cdot|_{1/2,*}$ is a norm on \widetilde{W}_h). We recall that, while in two dimensions the space \widetilde{W}_h can be defined as the subspace of functions continuous at the vertices of the subdomains, it is known that this is not sufficient to get a quasi-optimal result in the three dimensional case, so that we also need to impose continuity of either edge or face averages (or both). While later in the paper we will analyze the different possible choices, for now we will only assume that a_h is coercive on \widetilde{W}_h .

Following the approach of [18], we introduce the operators $\widehat{\mathcal{S}} : \widehat{W}_h \rightarrow \widehat{W}'_h$ and $\widetilde{\mathcal{S}} : \widetilde{W}_h \rightarrow \widetilde{W}'_h$ defined respectively as

$$(4.13) \quad \langle \widehat{\mathcal{S}} w_h, v_h \rangle = s(w_h, v_h) \quad \forall v_h \in \widehat{W}_h, \quad \langle \widetilde{\mathcal{S}} w_h, v_h \rangle = s(w_h, v_h) \quad \forall v_h \in \widetilde{W}_h,$$

and we let $\mathcal{R} : \widehat{W}_h \rightarrow \widetilde{W}_h$ denote the natural injection operator. We observe that

$$\widehat{\mathcal{S}} = \mathcal{R}^T \widetilde{\mathcal{S}} \mathcal{R}.$$

Problem 4.6 becomes

$$(4.14) \quad \widehat{\mathcal{S}}u = \widehat{g}.$$

with \widehat{f} suitable right-hand side.

Following [45], we let δ_ℓ denote the weighted counting function associated with $\partial\Omega^\ell$ and defined for $\gamma \in [1/2, \infty)$ by a sum of contribution from Ω^ℓ and its neighbors. More precisely, for $i \in \mathcal{Y}^\ell$, we set

$$(4.15) \quad \delta_\ell(y_i) = \frac{\sum_{j \in \mathcal{N}_i} \rho_j^\gamma}{\rho_\ell^\gamma}.$$

As in [34, 32], we define the scalar product $d : W_h \times W_h \rightarrow \mathbb{R}$ as

$$(4.16) \quad d(w_h, v_h) = \sum_\ell \sum_{i \in \mathcal{Y}^\ell} d^{\ell,i} v^\ell(y_i) w^\ell(y_i),$$

where, for $i \in \mathcal{Y}^\ell$, the scaling coefficient $d^{\ell,i}$ is defined as

$$(4.17) \quad d^{\ell,i} = (\delta_\ell(y_i))^{-1} = \frac{\rho_\ell^\gamma}{\sum_{j \in \mathcal{N}_i} \rho_j^\gamma}.$$

Next, we introduce the projection operator $\mathcal{E}_D : W_h \rightarrow \widehat{W}_h$, orthogonal with respect to the scalar product d :

$$(4.18) \quad d(\mathcal{E}_D w_h, v_h) = d(w_h, v_h), \quad \forall v_h \in \widehat{W}_h.$$

Following [18], we introduce the quotient space $\Sigma_h = \widetilde{W}_h / \widehat{W}_h$. We let $\Lambda_h = \Sigma'_h$ denote its dual and we let $\mathcal{B} : \widetilde{W}_h \rightarrow \Sigma_h = \Lambda'_h$ denote the quotient mapping, defined as

$$\mathcal{B}w_h = w_h + \widehat{W}_h.$$

Observe that two elements w_h and v_h are representative of the same equivalence class in Σ_h if and only if they have the same jump across the interface: for $F \in \mathcal{F}_H$ with $F = \Gamma^m \cap \Gamma^\ell$, $w_h^m - w_h^\ell = v_h^m - v_h^\ell$. We can then identify Σ_h with the set of jumps of elements of W_h . The quotient map \mathcal{B} can then be interpreted as the operator that maps an element of W_h to its jump on the interface. Clearly

$$\widehat{W}_h = \ker(\mathcal{B}) = \{w_h \in \widetilde{W}_h : b(w_h, \lambda) = 0, \quad \forall \lambda \in \Lambda_h\},$$

where $b : \widetilde{W}_h \times \Lambda_h \rightarrow \mathbb{R}$ is defined as $b(w_h, \lambda_h) = \langle \mathcal{B}w_h, \lambda_h \rangle$. Problem 2.3 is then equivalent to the following saddle point problem: find $w_h \in \widetilde{W}_h$, $\lambda_h \in \Lambda_h$ solution to

$$(4.19) \quad \widetilde{\mathcal{S}}w_h - \mathcal{B}^T \lambda_h = \widetilde{g}, \quad \mathcal{B}w_h = 0,$$

where $\widetilde{g} \in W'_h$ is defined by

$$\langle \widetilde{g}, w_h \rangle = \int_\Omega g \mathcal{L}_h w_h = \sum_\ell \int_{\Omega^\ell} g \mathcal{L}_h^\ell w_h^\ell.$$

Using the first equation in (4.19) to express w_h as a function of λ_h , we eliminate the former unknown and finally reduce the solution of Problem 4.6 to the solution of a problem in the unknown $\lambda_h \in \Lambda_h$ of the form

$$(4.20) \quad \mathcal{B} \widetilde{\mathcal{S}}^{-1} \mathcal{B}^T \lambda_h = -\mathcal{B} \widetilde{\mathcal{S}}^{-1} \widetilde{f}.$$

Letting now $\mathcal{B}^+ : \Sigma_h \rightarrow \widetilde{W}_h$ be any right inverse of \mathcal{B} (for $\eta \in \Sigma_h$, $\mathcal{B}^+\eta$ is any element in \widetilde{W}_h such that $\mathcal{B}\mathcal{B}^+\eta = w_h$), we set

$$\mathcal{B}_D^T = (\mathbf{1}_{\widetilde{W}_h} - \mathcal{E}_D)\mathcal{B}^+,$$

where $\mathbf{1}_{\widetilde{W}_h}$ denotes the identity operator in the space \widetilde{W}_h . Recall that, as in the two dimensional case, the definition of \mathcal{B}_D^T is independent of the actual choice of the operator \mathcal{B}^+ . Indeed $\mathcal{B}(\mathcal{B}_1^+\eta - \mathcal{B}_2^+\eta) = \eta - \eta = 0$ implies $\mathcal{B}_1^+\eta - \mathcal{B}_2^+\eta \in \widetilde{W}_h$ and hence $(\mathbf{1}_{\widetilde{W}_h} - \mathcal{E}_D)\mathcal{B}_1^+\eta - (\mathbf{1}_{\widetilde{W}_h} - \mathcal{E}_D)\mathcal{B}_2^+\eta = 0$.

We finally let the FETI preconditioner $\mathcal{M} : \Sigma_h \rightarrow \Lambda_h$ be defined by

$$(4.21) \quad \mathcal{M} = \mathcal{B}_D \widetilde{\mathcal{S}} \mathcal{B}_D^T.$$

Let us now come to the choice of the space \widetilde{W}_h , or, equivalently, to the choice of the so called *primal* degrees of freedom, which are taken as single valued, thus directly imposing the corresponding degree of continuity across the interface, whereas continuity for the remaining *dual* degrees of freedom is imposed via Lagrange multipliers in Λ_h . Exactly as in the finite element case there are several possibilities. Letting

$$(4.22) \quad \begin{aligned} \widetilde{W}_h^V &= \{w_h \in W_h : w_h^\ell(y_i) = w_h^m(y_i), \forall i \in \mathcal{X}, \ell, m \in \mathcal{N}_i\}, \\ \widetilde{W}_h^E &= \{w_h \in W_h : \int_E w_h^\ell = \int_E w_h^k, \forall E \in \mathcal{E}_H, \ell, k \in \mathcal{N}_E\}, \\ \widetilde{W}_h^F &= \{w_h \in W_h : \int_F w_h^\ell = \int_F w_h^k, \forall F \in \mathcal{F}_H, \ell, k \in \mathcal{N}_F\}, \end{aligned}$$

denote the subset of W_h of traces of functions which, respectively, are continuous at cross-points, have same average at all edges, and have same average at all faces, different choices for \widetilde{W}_h can be considered, see Section 6, resulting in different versions of the FETI algorithms. More precisely we have

$$\begin{aligned} \text{E: } \widetilde{W}_h &= \widetilde{W}_h^E \text{ (primal d.o.f.'s are the edge averages);} \\ \text{F: } \widetilde{W}_h &= \widetilde{W}_h^F \text{ (primal d.o.f.'s are the face averages);} \\ \text{VE: } \widetilde{W}_h &= \widetilde{W}_h^V \cap \widetilde{W}_h^E \text{ (primal d.o.f.'s are the values at cross points and the edge averages);} \\ \text{VF: } \widetilde{W}_h &= \widetilde{W}_h^V \cap \widetilde{W}_h^F \text{ (primal d.o.f.'s are the values at cross points and the face averages);} \\ \text{EF: } \widetilde{W}_h &= \widetilde{W}_h^E \cap \widetilde{W}_h^F \text{ (primal d.o.f.'s are edge and face averages);} \\ \text{VEF: } \widetilde{W}_h &= \widetilde{W}_h^V \cap \widetilde{W}_h^E \cap \widetilde{W}_h^F \text{ (primal d.o.f.'s are the values at cross points and the face and edge averages).} \end{aligned}$$

As it happens for the finite element case, all the above choices lead to a quasi-optimal (in terms of dependence on h and H) preconditioning, whereas robustness with respect to the jumps in the coefficient ρ is achieved for algorithms VE and VEF, as stated by the following theorem.

Theorem 4.7. *Letting κ denote the condition number of the matrix corresponding to the operator $\mathcal{M}(\mathcal{B}\widetilde{\mathcal{S}}^{-1}\mathcal{B}^T)$, depending on the choice of the space \widetilde{W}_h we have the following bounds:*

Algorithms E / EF: *If $\widetilde{W}_h \subseteq \widetilde{W}_h^E$ then*

$$\kappa \lesssim \left(1 + \log\left(\frac{H}{h}\right) + \tau_E\right) \left(1 + \log\left(\frac{H}{h}\right)\right);$$

Algorithm F: If $\widetilde{W}_h \subseteq \widetilde{W}_h^F$ then

$$\kappa \lesssim \left(1 + \log\left(\frac{H}{h}\right) + \tau_F\right) \left(1 + \log\left(\frac{H}{h}\right)\right);$$

Algorithms VE / VEF: If $\widetilde{W}_h \subseteq \widetilde{W}_h^V \cap \widetilde{W}_h^E$ then

$$\kappa \lesssim \left(1 + \log\left(\frac{H}{h}\right)\right)^2;$$

Algorithm VF: If $\widetilde{W}_h \subseteq \widetilde{W}_h^V \cap \widetilde{W}_h^F$ then

$$\kappa \lesssim \left(1 + \log\left(\frac{H}{h}\right) + \tau_{EF}\right) \left(1 + \log\left(\frac{H}{h}\right)\right),$$

where τ_E , τ_F and τ_{EF} are constants depending on the diffusion coefficient ρ that satisfy

$$(4.23) \quad 0 < \tau_E, \tau_F, \tau_{EF} \leq \max \rho / \min \rho, \quad \tau_E \leq \tau_F, \quad \tau_{EF} \leq \tau_F.$$

Remark 4.8. The precise definition of the constant τ_E , τ_F and τ_{EF} (which will be detailed in Section 5) is the same as in the finite element case [45], and it is quite technical. We would like to remark that the bounds (4.23) are often quite pessimistic, as we will see in Section 6

4.2. Implementation in the Virtual Element context. As in the Finite Element case, the implementation of the FETI-DP method entails the need for numerically imposing the continuity constraints on the primal degrees of freedom, either directly or via additional Lagrange multipliers (using which, the computation of \widetilde{S}^{-1} will imply solving an algebraic saddle point problem) [32]. In order to do this, it is necessary to be able to evaluate the primal degrees of freedom for any given discrete functions, and, if imposing the continuity directly, to explicitly construct a basis function for each primal degree of freedom, being it a vertex value, an edge average, or a face average. While for vertex and edge degrees of freedom this is not difficult, the same is not true for face averages. Indeed, contrary to what happens for finite elements, discrete functions are explicitly known only on the edges of the tessellation, where they are linear. On faces and within the elements VEM basis functions are not explicitly known and all quantities needed for the implementation (of the preconditioner, but also of the stiffness matrix and load vector) have to be retrieved in terms of the values at the nodes and on the edges, by exploiting the definitions of the spaces $V^{1,f}$ and $V^{1,K}$ (in the terminology of VEM, they must be *computable*). Extended details on the computability of the stiffness matrix and the right hand side can be found in [7]. Here we concentrate on the quantities needed for implementing the FETI-DP method, and, more specifically, on the face averages of discrete functions. Let $w_h^\ell \in W_h^\ell$ and let F denote a macro face of Ω^ℓ . We observe that F can be written as the union of a certain number of faces f of polyhedra of the tessellation \mathcal{T}_h . We have then

$$|F|^{-1} \int_F w_h = |F|^{-1} \sum_{f \subset F} \int_f w_h = |F|^{-1} \sum_{f \subset F} \int_f \Pi_f^\nabla w_h,$$

where the last identity stems from the definition (2.2) of the space $V^{f,1}$ to which $w_{h|f}$ belongs. We recall that, thanks to (2.4), $\Pi_f^\nabla w_h$ is computable in terms of the (known) value of w_h on ∂f .

Implementation of the FETI-DP preconditioner can then be carried out following different approaches [32]. As already stated, continuity of the primal variables can be imposed directly by explicitly constructing a basis allowing to decoupling the primal variables, for which continuity is strongly imposed, from the dual variables, or by introducing additional Lagrange multipliers. For the numerical experiments that we present in Section 6, we chose the first option, which leads to smaller and computationally more efficient coarse problems.

5. PROOF OF THEOREM 4.7

We start by remarking that, by construction, we are in the framework of [35]. In particular we have the identity

$$\mathcal{B}_D^T \mathcal{B} + \mathcal{E}_D = \mathbf{1}_{\widetilde{W}_h}.$$

In fact, it is not difficult to see that for all $w_h \in \widetilde{W}_h$ we have that $(\mathbf{1}_{\widetilde{W}_h} - \mathcal{B}_D^T \mathcal{B})w_h \in \widehat{W}_h$ and that we have

$$d((\mathbf{1}_{\widetilde{W}_h} - \mathcal{B}_D^T \mathcal{B})w_h, v_h) = d(w_h, v_h) \quad \text{for all } v_h \in \widehat{W}_h.$$

Then we have ([35])

$$(5.1) \quad \kappa \lesssim \max_{w_h \in \widetilde{W}_h} \frac{s(\mathcal{B}_D^T \mathcal{B} w_h, \mathcal{B}_D^T \mathcal{B} w_h)}{s(w_h, w_h)} \simeq \max_{w_h \in \widetilde{W}_h} \frac{s(\mathcal{E}_D w_h, \mathcal{E}_D w_h)}{s(w_h, w_h)}.$$

In order to have a bound on the condition number, we then only need to bound $s(\mathcal{E}_D w_h, \mathcal{E}_D w_h)$ in terms of $s(w_h, w_h)$.

To start, let us recall some functional inequalities that will be useful in the following. Let F be a shape regular polygon (in the following F will be a face of one of the Ω^ℓ 's). Then, for all $\eta \in H^s(F)$, $1/2 < s \leq 1$, we have, uniformly in s , the following trace inequalities

$$(5.2) \quad \|\eta\|_{H^{s-1/2}(\partial F)} \lesssim \frac{1}{\sqrt{2s-1}} \|\eta\|_{H^s(F)}, \quad |\eta|_{H^{s-1/2}(\partial F)} \lesssim \frac{1}{\sqrt{2s-1}} |\eta|_{H^s(F)}.$$

On the other hand, for all $\eta \in H^s(F)$, $0 \leq s < 1/2$, and for all $\alpha \in \mathbb{R}$ it holds that

$$(5.3) \quad \|u\|_{H_0^s(F)} \lesssim \frac{1}{1/2-s} \|u - \alpha\|_{H^s(F)} + \frac{1}{\sqrt{1/2-s}} |\alpha|,$$

once again uniformly in s (recall that we are using scaled norms, as defined in Section 2, so that the bounds are uniform in H).

We also observe that, thanks to the inverse inequality (3.3) and to the scaling of the norms, by using a standards space interpolation technique it is not difficult to prove that for all $r, s \in [0, 1]$ with $r < s$, and for all $w_h \in W_{h|F}$

$$(5.4) \quad \|w_h\|_{H^s(F)} \lesssim \left(\frac{H}{h}\right)^{r-s} \|w_h\|_{H^r(F)}.$$

An analogous bound holds for the norms in the spaces $H_0^s(F)$ and $H_0^r(F)$ (with the usual care when either s or r are equals to $1/2$), provided $w_h \in W_{h|F} \cap H_0^1(F)$. In particular, in such case we have

$$(5.5) \quad \|w_h\|_{H_0^{1/2}(F)} \lesssim \left(\frac{H}{h}\right)^{r-s} \|w_h\|_{H_0^r(F)}.$$

The following proposition holds.

Proposition 5.1. *Let Ω^ℓ be a shape regular subdomain and let F be a face of Ω^ℓ . Then for $w_h \in W_{h|F}$ we have*

$$\|w_h\|_{L^2(\partial F)} \lesssim \sqrt{1 + \log(h/H)} \|w_h\|_{H^{1/2}(F)}.$$

Proof. Using inequalities (5.4) and (5.2) we can write, for $0 < \varepsilon \leq 1/2$ arbitrary,

$$\begin{aligned} \|w_h\|_{L^2(\partial F)} &\leq \|w_h\|_{H^\varepsilon(\partial F)} \lesssim \frac{1}{\sqrt{\varepsilon}} \|w_h\|_{H^{1/2+\varepsilon}(F)} \lesssim \\ &\lesssim \left(\frac{h}{H}\right)^{-\varepsilon} \frac{1}{\sqrt{\varepsilon}} \|w_h\|_{H^{1/2}(F)} \lesssim \sqrt{1 + \log(h/H)} \|w_h\|_{H^{1/2}(F)}, \end{aligned}$$

where the last bound is obtained by choosing $\varepsilon = (1 + \log(H/h))^{-1}$. \square

We now prove the following lemma, which is the equivalent, for the Virtual Element Method, of Lemma 5.6 of [43] and Lemma 4.3 of [17].

Lemma 5.2. *Let $w_h \in W_h^\ell$ and let $\hat{w}_h \in W_h^\ell$ be defined by $\hat{w}_h(y_i) = 0$, for all $i \in \mathcal{W}^\ell$, $\hat{w}_h(y_i) = w_h(y_i)$, for all $i \in \mathcal{Y}^\ell \setminus \mathcal{W}^\ell$. Then, for all face F of Ω_ℓ it holds that*

$$\|\hat{w}_h\|_{H_{00}^{1/2}(F)}^2 \lesssim (1 + \log(H/h))^2 \|w_h\|_{H^{1/2}(F)}^2.$$

Moreover, if w_h is constant on F then

$$\|\hat{w}_h\|_{H_{00}^{1/2}(F)}^2 \lesssim (1 + \log(H/h)) \|w_h\|_{H^{1/2}(F)}^2$$

Proof. We let \hat{W}_h^F be defined as

$$\hat{W}_h^F = \{w_h \in W_h^F = V_h|_F : w_h(y_i) = 0 \text{ for all } i \in \mathcal{W}_F\}.$$

Let $\pi_h : L^2(F) \rightarrow W_h^F$ and $\pi_h^0 : L^2(F) \rightarrow \hat{W}_h^F$ denote the L^2 -projection onto W_h^F and onto \hat{W}_h^F , respectively. Recall that for all $u \in H^1(F)$, using (4.8) we have

$$(5.6) \quad \|u - \pi_h u\|_{L^2(F)} \leq \|u - \Pi_{SZ} u\|_{L^2(F)} \lesssim \frac{h}{H} |u|_{H^1(F)},$$

and, since $u \in H_0^1(F)$ implies that $\Pi_{SZ} u \in \hat{W}_h^F$, we also have for all $u \in H_0^1(F)$

$$(5.7) \quad \|u - \pi_h^0 u\|_{L^2(F)} \leq \|u - \Pi_{SZ} u\|_{L^2(F)} \lesssim \frac{h}{H} |u|_{H^1(F)}.$$

Let now $i_h^0 : W_h^F \rightarrow \hat{W}_h^F$ be defined by $i_h^0 w_h(y_i) = w_h(y_i)$ for all $i \in \mathcal{Y}_F \setminus \mathcal{W}_F$, so that, on F , $\hat{w}_h^\ell = i_h^0 w_h$. Remark that, thanks to Lemma 3.1, we have

$$(5.8) \quad \|i_h^0 w_h\|_{L^2(F)}^2 \lesssim \left(\frac{h}{H}\right)^2 \sum_{i \in \mathcal{Y}_F \setminus \mathcal{W}_F} |w_h(y_i)|^2 \lesssim \left(\frac{h}{H}\right)^2 \sum_{i \in \mathcal{Y}_F} |w_h(y_i)|^2 \lesssim \|w_h\|_{L^2(F)}^2.$$

Consider now the operator $\pi_h^1 = i_h^0 \circ \pi_h : L^2(F) \rightarrow \hat{W}_h^F$ obtained by first projecting onto W_h^F and then setting the values at nodes on ∂F to zero. We will prove that the restriction of π_h^1 to $H_0^s(F)$ is uniformly bounded for all $s < 1/2$, that is, that for all $w \in H_0^s(F)$ we have

$$(5.9) \quad \|\pi_h^1 w\|_{H_0^s(F)} \lesssim \|w\|_{H_0^s(F)},$$

with a constant independent of s . Then, for $\varepsilon \in]0, 1/2[$ arbitrary, using (5.5) and (5.3), we can write

$$\begin{aligned} \|\pi_h^1 w_h\|_{H_{00}^{1/2}(F)} &\lesssim \left(\frac{h}{H}\right)^{-\varepsilon} \|\pi_h^1 w_h\|_{H_0^{1/2-\varepsilon}(F)} \lesssim \left(\frac{h}{H}\right)^{-\varepsilon} \|w_h\|_{H_0^{1/2-\varepsilon}(F)} \lesssim \\ &\lesssim \frac{1}{\varepsilon} \left(\frac{h}{H}\right)^{-\varepsilon} \|w_h\|_{H^{1/2-\varepsilon}(F)} \lesssim (1 + \log(H/h)) \|w_h\|_{H^{1/2}(F)}, \end{aligned}$$

which by choosing $\varepsilon = 1/|\log(H/h)|$, yields

$$\|\pi_h^1 w_h\|_{H_0^1(F)} \lesssim (1 + \log(H/h)) \|w_h\|_{H^1(F)}.$$

Observing that for $w_h \in W_h^F$ we have

$$\dot{w}_h^\ell|_E = i_h^0 w_h|_E = \pi_h^1 w_h|_E,$$

we immediately get the thesis (the result for w_h^ℓ constant on F is obtained by setting $\alpha = w_h^\ell$ in (5.3)).

Let us then prove (5.9). We easily see that π_h^1 is L^2 bounded: for all $w \in L^2(F)$,

$$\|\pi_h^1 w\|_{L^2(F)} \lesssim \|\pi_h w\|_{L^2(F)} \lesssim \|w\|_{L^2(F)}.$$

On the other hand, observing that $i_h^0 \circ \pi_h^0 = \pi_h^0$, using (5.8) we see that, for $w \in H_0^1(F)$

$$\|w - \pi_h^1 w\|_{L^2(F)} = \|w - \pi_h^0 w + i_h^0 \pi_h^0 w - i_h^0 \pi_h w\|_{L^2(F)} \lesssim \|w - \pi_h^0 w\|_{L^2(F)} + \|\pi_h^0 w - \pi_h w\|_{L^2(F)}.$$

By adding and subtracting w in the second term on the right hand side and using (5.6) and (5.7), we obtain, for $w \in H_0^1(F)$,

$$\|w - \pi_h^1 w\|_{L^2(F)} \lesssim \|w - \pi_h^0 w\|_{L^2(F)} + \|w - \pi_h w\|_{L^2(F)} \lesssim \frac{h}{H} |w|_{H^1(F)}.$$

This allows us to prove, by a standard argument, that π_h^1 is H_0^1 -bounded. In fact, letting $\Pi_h^1 : H_0^1(F) \rightarrow \dot{W}_h^F$ denote the H_0^1 projection, for $w \in H_0^1(F)$, using an inverse inequality, adding and subtracting w and then using an approximation bound, we have

$$\begin{aligned} |\pi_h^1 w|_{H^1(F)} &= |\Pi_h^1 w|_{H^1(F)} + |\pi_h^1 w - \Pi_h^1 w|_{H^1(F)} \lesssim |w|_{H^1(F)} + \left(\frac{h}{H}\right)^{-1} \|\pi_h^1 w - \Pi_h^1 w\|_{L^2(F)} \lesssim \\ &\lesssim |w|_{H^1(F)} + \left(\frac{h}{H}\right)^{-1} \|\pi_h^1 w - w\|_{L^2(F)} + \left(\frac{h}{H}\right)^{-1} \|w - \Pi_h^1 w\|_{L^2(F)} \lesssim \\ &\lesssim |w|_{H^1(F)} + \left(\frac{h}{H}\right)^{-1} \left(\frac{h}{H}\right) |w|_{H^1(F)} + \left(\frac{h}{H}\right)^{-1} \left(\frac{h}{H}\right) |w|_{H^1(F)} \lesssim |w|_{H^1(F)}. \end{aligned}$$

The bound (5.9) follows by a standard space interpolation argument. \square

Let us now consider the projector $\mathcal{E}_D : W_h \rightarrow \widehat{W}_h$. We have the following Lemma.

Lemma 5.3. *For all $w_h \in W_h$ it holds that*

$$(5.10) \quad |\mathcal{E}_D w_h|_{1/2,*}^2 \lesssim (1 + \log(H/h))^2 |w_h|_{1/2,*}^2 + \left(\frac{h}{H}\right) \Delta^{\mathcal{X}} + \Delta^{\mathcal{E}} + (1 + \log(H/h)) \Delta^{\mathcal{F}},$$

with

$$(5.11) \quad \Delta^{\mathcal{X}} = \sum_{i \in \mathcal{X}} \sum_{\ell, k \in \mathcal{N}_i} \min\{\rho_\ell, \rho_k\} |w_h^\ell(y_i) - w_h^k(y_i)|^2,$$

$$(5.12) \quad \Delta^{\mathcal{E}} = \sum_{E \in \mathcal{E}_H} \sum_{\ell, k \in \mathcal{N}_E} \min\{\rho_\ell, \rho_k\} |\alpha_\ell^E - \alpha_k^E|^2,$$

$$(5.13) \quad \Delta^{\mathcal{F}} = \sum_{F \in \mathcal{F}_H} \sum_{\ell, k \in \mathcal{N}_F} \min\{\rho_\ell, \rho_k\} |\alpha_\ell^F - \alpha_k^F|^2,$$

where

$$(5.14) \quad \alpha_\ell^F = |F|^{-1} \int_F w_h^\ell, \quad \alpha_\ell^E = |E|^{-1} \int_E w_h^\ell.$$

Proof. It is not difficult to check that, for $i \in \mathcal{Y}$ we have

$$\mathcal{E}_D w_h(y_i) = \theta_i^{-1} \sum_{k \in \mathcal{N}_i} \rho_k^\gamma w_h^k(y_i), \quad \text{where } \theta_i = \sum_{k \in \mathcal{N}_i} \rho_k^\gamma,$$

and that these relations completely define \mathcal{E}_D .

Let both w_h and $v_h = \mathcal{E}_D w_h$ be split as the sum of the contributions of nodes on the wirebasket, which we will denote by w_h^\sharp and v_h^\sharp , respectively, and the contribution of nodes interior to the faces, which we will denote by \hat{w}_h and \hat{v}_h , respectively. More precisely, we let $w_h^\sharp \in W_h$ and $v_h^\sharp \in \widehat{W}_h$ be defined by

$$w_h^\sharp = (w_h^{\ell, \sharp})_\ell \text{ with } w_h^{\ell, \sharp}(y_i) = \begin{cases} w_h^\ell(y_i), & i \in \mathcal{W}^\ell, \\ 0, & i \in \mathcal{Y}^\ell \setminus \mathcal{W}^\ell, \end{cases} \quad \text{and} \quad v_h(y_i) = \begin{cases} v_h(y_i) & i \in \mathcal{W}, \\ 0 & i \in \mathcal{Y} \setminus \mathcal{W}, \end{cases}$$

and we set $\hat{w}_h = w_h - w_h^\sharp$ and $\hat{v}_h = v_h - v_h^\sharp$. Remark that

$$v_h^\sharp = \mathcal{E}_D w_h^\sharp, \quad \hat{v}_h = \mathcal{E}_D \hat{w}_h.$$

To start, let us consider the contribution of the faces. We have

$$\rho_\ell |\hat{v}_h|_{H^{1/2}(\partial\Omega_\ell)}^2 \lesssim \rho_\ell \sum_{F \in \mathcal{F}_H^\ell} \|\hat{v}_h\|_{H_0^{1/2}(F)}^2.$$

We recall that for $a, b > 0$ and $\gamma \geq 1/2$ we have $ab^{2\gamma}/(a^\gamma + b^\gamma)^2 \lesssim \min\{a, b\}$. Let F be the common face of the subdomains Ω^ℓ and Ω^k . On F we have $\mathcal{E}_D \hat{w}_h = \theta_F^{-1} (\rho_\ell^\gamma \hat{w}_h^\ell + \rho_k^\gamma \hat{w}_h^k)$ where $\theta_F = \rho_\ell^\gamma + \rho_k^\gamma$. Letting $\Theta_F \in \widehat{W}_h^F$ denote the function defined by

$$\Theta_F(y_i) = 1 \quad \forall i \in \mathcal{Y}_F \setminus \mathcal{W}_F, \quad \Theta_F(y_i) = 0 \quad \forall i \in \mathcal{W}_F,$$

we can write

$$\begin{aligned} \rho_\ell \|\hat{w}_h^\ell - \hat{v}_h\|_{H_0^{1/2}(F)}^2 &= \rho_\ell (\theta_F^{-1} \rho_k^\gamma)^2 \|\hat{w}_h^\ell - \hat{w}_h^k\|_{H_0^{1/2}(F)}^2 \\ &\lesssim \min\{\rho_\ell, \rho_k\} \|\hat{w}_h^\ell - \alpha_\ell^F \Theta_F + \alpha_k^F \Theta_F - \hat{w}_h^k\|_{H_0^{1/2}(F)}^2 + \min\{\rho_\ell, \rho_k\} \|(\alpha_\ell^F - \alpha_k^F) \Theta_F\|_{H_0^{1/2}(F)}^2 \\ &\lesssim \rho_\ell \|\hat{w}_h^\ell - \alpha_\ell^F \Theta_F\|_{H_0^{1/2}(F)}^2 + \rho_k \|\hat{w}_h^k - \alpha_k^F \Theta_F\|_{H_0^{1/2}(F)}^2 + \min\{\rho_\ell, \rho_k\} \|(\alpha_\ell^F - \alpha_k^F) \Theta_F\|_{H_0^{1/2}(F)}^2. \end{aligned}$$

We now apply Lemma 5.2, which, thanks to Poincaré inequality, gives us

$$\begin{aligned} \rho_\ell \|\hat{w}_h^\ell - \hat{v}_h\|_{H_0^{1/2}(F)}^2 &\lesssim (1 + \log(H/h))^2 \left(\rho_\ell |w_h^\ell|_{H^{1/2}(F)}^2 + \rho_k |w_h^k|_{H^{1/2}(F)}^2 \right) \\ &\quad + \min\{\rho_\ell, \rho_k\} (1 + \log(H/h)) |\alpha_\ell^F - \alpha_k^F|^2. \end{aligned}$$

Adding up over all subdomains and over all faces (each face is counted twice) we obtain

$$|\hat{w}_h - \hat{v}_h|_{1/2, *}^2 \lesssim (1 + \log(H/h))^2 |w_h|_{1/2, *}^2 + (1 + \log(H/h)) \Delta^{\mathcal{F}}.$$

We now consider the contribution of the wirebasket. Using an inverse inequality analogous to (5.4), and Lemma 3.1, we can write

$$(5.15) \quad \rho_\ell |w_h^{\ell, \#} - v_h^\#|_{H^{1/2}(\partial\Omega^\ell)}^2 \lesssim \rho_\ell \left(\frac{h}{H}\right)^{-1} \|w_h^{\ell, \#} - v_h^\#\|_{L^2(\partial\Omega^\ell)}^2 \lesssim \rho_\ell \left(\frac{h}{H}\right) \sum_{i \in \mathcal{W}^\ell} |w_h^\ell(y_i) - v_h(y_i)|^2.$$

We can write

$$(5.16) \quad \begin{aligned} \rho_\ell |w_h^\ell(y_i) - v_h(y_i)|^2 &= \rho_\ell |\theta_i^{-1} \sum_{k \in \mathcal{N}_i} \rho_k^\gamma (w_h^\ell(y_i) - w_h^k(y_i))|^2 \\ &\lesssim \sum_{k \in \mathcal{N}_i} \rho_\ell (\theta_i^{-1} \rho_k^\gamma)^2 |w_h^\ell(y_i) - w_h^k(y_i)|^2 \lesssim \sum_{k \in \mathcal{N}_i} \min\{\rho_\ell, \rho_k\} |w_h^\ell(y_i) - w_h^k(y_i)|^2. \end{aligned}$$

Plugging (5.16) in (5.15) and adding up over all ℓ we obtain

$$(5.17) \quad \begin{aligned} |w_h^\# - v_h^\#|_{1/2, *}^2 &\lesssim \left(\frac{h}{H}\right) \sum_\ell \sum_k \sum_{i \in \mathcal{W}^k \cap \mathcal{W}^\ell} \min\{\rho_\ell, \rho_k\} |w_h^\ell(y_i) - w_h^k(y_i)|^2 \lesssim \\ &\left(\frac{h}{H}\right) \Delta^\mathcal{X} + \sum_{E \in \mathcal{E}_H} \sum_{\ell, k \in \mathcal{N}_E} \left(\frac{h}{H}\right) \sum_{i \in \mathcal{Y}_E} \min\{\rho_\ell, \rho_k\} |w_h^\ell(y_i) - w_h^k(y_i)|^2. \end{aligned}$$

Now, given $E \in \mathcal{E}_H$, for $\ell, k \in \mathcal{N}_E$ and $i \in \mathcal{Y}_E$ we can write

$$\min\{\rho_\ell, \rho_k\} |w_h^\ell(y_i) - w_h^k(y_i)|^2 \lesssim \rho_\ell |w_h^\ell(y_i) - \alpha_\ell^E|^2 + \rho_k |w_h^k(y_i) - \alpha_k^E|^2 + \min\{\rho_\ell, \rho_k\} |\alpha_\ell^E - \alpha_k^E|^2,$$

yielding

$$(5.18) \quad \begin{aligned} \left(\frac{h}{H}\right) \sum_{i \in \mathcal{Y}_E} \min\{\rho_\ell, \rho_k\} |w_h^\ell(y_i) - w_h^k(y_i)|^2 &\lesssim \left(\frac{h}{H}\right) \sum_{i \in \mathcal{Y}_E} \rho_\ell |w_h^\ell(y_i) - \alpha_\ell^E|^2 \\ &+ \left(\frac{h}{H}\right) \sum_{i \in \mathcal{Y}_E} \rho_k |w_h^k(y_i) - \alpha_k^E|^2 + \left(\frac{h}{H}\right) \min\{\rho_\ell, \rho_k\} \#(\mathcal{Y}_E) |\alpha_\ell^E - \alpha_k^E|^2 \\ &\lesssim \rho_\ell \|w_h^\ell - \alpha_\ell^E\|_{L^2(E)}^2 + \rho_k \|w_h^k - \alpha_k^E\|_{L^2(E)}^2 + \min\{\rho_\ell, \rho_k\} |\alpha_\ell^E - \alpha_k^E|^2, \end{aligned}$$

where we used Lemma 3.1 and the fact that, under the assumptions made on the tessellation, we have that $\#(\mathcal{Y}_E) \lesssim H/h$. Then

$$|w_h^\# - v_h^\#|_{1/2, *}^2 \lesssim \left(\frac{h}{H}\right) \Delta^\mathcal{X} + \Delta^\mathcal{E} + \sum_E \sum_{\ell \in \mathcal{N}_E} \rho_\ell \|w_h^\ell - \alpha_\ell^E\|_{L^2(E)}^2.$$

We conclude by observing that

$$\sum_E \sum_{\ell \in \mathcal{N}_E} \rho_\ell \|w_h^\ell - \alpha_\ell^E\|_{L^2(E)}^2 \lesssim \sum_\ell \sum_{F \in \mathcal{F}_H^\ell} \rho_\ell \|w_h^\ell - \alpha_\ell^F\|_{L^2(\partial F)}^2$$

(we used that α_ℓ^E minimizes $\|w_h^\ell - \alpha\|_{L^2(E)}$). Applying Proposition 5.1 we then obtain

$$\sum_E \sum_{\ell \in \mathcal{N}_E} \rho_\ell \|w_h^\ell - \alpha_\ell^E\|_{L^2(E)}^2 \lesssim (1 + \log(h/H)) \|w_h - \alpha^F\|_{1/2, *}^2 \lesssim (1 + \log(h/H)) |w_h|_{1/2, *}^2.$$

□

Observe that $\Delta^\mathcal{X}$, $\Delta^\mathcal{E}$ and $\Delta^\mathcal{F}$ vanish provided that w_h belongs to \widetilde{W}^V , \widetilde{W}^E and \widetilde{W}^F , respectively, so that, depending on the choice of \widetilde{W}_h , some of the terms at the right hand side of (5.10) disappear. In order to get a bound for \mathcal{E}_D for the different choices of \widetilde{W}_h , we then need to bound the remaining

terms in the different cases. We start by comparing, for a given function w_h , the average over a face with the average over one of its edges.

Lemma 5.4. *For E edge of $F \subset \partial\Omega^\ell$ it holds that*

$$(5.19) \quad |\alpha_\ell^E - \alpha_\ell^F|^2 \lesssim (1 + \log(h/H)) |w_h^\ell|_{H^{1/2}(F)}^2.$$

Proof. Let π_E denote the $L^2(E)$ projection onto constant functions, which is defined by

$$\pi_E w = |E|^{-1} \int_E w.$$

Thanks to the trace inequality (5.2) it holds that

$$\|\pi_E w\|_{L^2(E)} \leq \|w\|_{L^2(E)} \leq \|w\|_{L^2(\partial F)} \lesssim \|w\|_{H^s(\partial F)} \lesssim \frac{1}{\sqrt{2s-1}} \|w\|_{H^s(F)}.$$

Trivially, such an operator preserves the constants. Then, by using Proposition 5.1 and a Poincaré type inequality, we can write

$$|\alpha_\ell^E - \alpha_\ell^F|^2 \simeq \|\pi_E(w_h^\ell - \alpha_\ell^F)\|_{L^2(E)}^2 \leq \|w_h^\ell - \alpha_\ell^F\|_{L^2(E)}^2 \lesssim (1 + \log(h/H)) |w_h^\ell|_{H^{1/2}(F)}^2.$$

□

We can now bound $\Delta^{\mathcal{X}}$ in terms of either $\Delta^{\mathcal{E}}$ or $\Delta^{\mathcal{F}}$.

Lemma 5.5. *The following inequalities hold*

$$(5.20) \quad \left(\frac{h}{H}\right) \Delta^{\mathcal{X}} \lesssim \tau_E \left((1 + \log(H/h)) |w_h|_{1/2,*}^2 + \Delta^{\mathcal{E}} \right),$$

$$(5.21) \quad \left(\frac{h}{H}\right) \Delta^{\mathcal{X}} \lesssim \tau_F (1 + \log(H/h)) \left(|w_h|_{1/2,*}^2 + \Delta^{\mathcal{F}} \right),$$

with τ_E, τ_F constants depending on the diffusion coefficient ρ , satisfying $0 < \tau_E \leq \tau_F \leq \max \rho / \min \rho$.

Proof. We start by proving (5.20). Let $i \in \mathcal{X}$ and let $\ell, k \in \mathcal{N}_i$. Assume at first that Ω^ℓ and Ω^k share an edge E having y_i as one of the vertices. Adding and subtracting $(\alpha_\ell^E - \alpha_k^E)$, using Proposition 5.1 as well as a Poincaré inequality for function with vanishing average in a portion of the boundary (allowing to bound the $H^{1/2}$ norm with the $H^{1/2}$ seminorm), we can write

$$\begin{aligned} & \left(\frac{h}{H}\right) \min\{\rho_\ell, \rho_k\} |w_h^\ell(y_i) - w_h^k(y_i)|^2 \lesssim \min\{\rho_\ell, \rho_k\} \|w_h^\ell - w_h^k\|_{L^2(E)}^2 \lesssim \\ & \lesssim (1 + \log(h/H)) (\rho_\ell |w_h^\ell|_{H^{1/2}(\partial\Omega^\ell)}^2 + \rho_k |w_h^k|_{H^{1/2}(\partial\Omega^k)}^2) + \min\{\rho_\ell, \rho_k\} |\alpha_\ell^E - \alpha_k^E|^2. \end{aligned}$$

Let now $\ell, k \in \mathcal{N}_i$ be two subdomains sharing a vertex y_i but not an edge. In this case we bound $|w_h^\ell(y_i) - w_h^k(y_i)|$ by adding and subtracting a suitable sequence of values $w_h^{n_i}(y_i)$ in such a way that we fall back in the previous case. To this aim we start by introducing the following definitions:

- a *path* \mathcal{P} of length N is any sequence of subdomains $\Omega^{n_0}, \dots, \Omega^{n_N}$ such that for all i , Ω^{n_i} and $\Omega^{n_{i+1}}$ share at least a vertex.
- for a given path $\mathcal{P} = (\Omega^{n_0}, \dots, \Omega^{n_N})$ we set $\tau_{\mathcal{P}} = (\min \rho_{n_i})^{-1}$, $i \in [0, \dots, N]$,
- a path $\mathcal{P} = (\Omega^{n_0}, \dots, \Omega^{n_N})$ *connects* Ω^ℓ and Ω^k *via edges* (resp. *via faces*) if $n_0 = \ell$, $n_N = k$ and for all $i = 1, \dots, N$ the subdomains Ω^{n_i} and $\Omega^{n_{i-1}}$ share an edge (resp. a face).

Letting K^* be the maximum number of subdomains sharing a vertex, we denote by $\mathbf{P}_E^{\ell,k}$ (resp. $\mathbf{P}_F^{\ell,k}$) the set of paths of length $\leq K^*$ connecting Ω^ℓ and Ω^k via edges (resp. via faces). For all

path $\mathcal{P} = (\Omega^{n_0}, \dots, \Omega^{n_N}) \in \mathbf{P}_E^{\ell,k}$ we can bound

$$\min\{\rho_\ell, \rho_k\} |w_h^\ell(y_i) - w_h^k(y_i)|^2 \lesssim \sum_{j=1}^N \frac{\min\{\rho_\ell, \rho_k\}}{\min\{\rho_{n_j}, \rho_{n_{j-1}}\}} \min\{\rho_{n_j}, \rho_{n_{j-1}}\} |w_h^{n_j}(y_i) - w_h^{n_{j-1}}(y_i)|^2$$

and, using the bound for subdomains sharing an edge, we obtain (5.20), with τ_E

$$\tau_E = \max_{(\ell,k): \Omega^\ell, \Omega^k \text{ share a vertex}} \left(\min\{\rho_\ell, \rho_k\} \tau_E^{\ell,k} \right)$$

where

$$\tau_E^{\ell,k} = \min_{\mathcal{P} \in \mathbf{P}_E^{\ell,k}} \tau_{\mathcal{P}}.$$

Bound (5.21) with $\tau_F^{\ell,k} = \min_{\mathcal{P} \in \mathbf{P}_F^{\ell,k}} \tau_{\mathcal{P}}$ and

$$\tau_F = \max_{(\ell,k): \Omega^\ell, \Omega^k \text{ share a vertex}} \left(\min\{\rho_\ell, \rho_k\} \tau_F^{\ell,k} \right)$$

is obtained by a similar argument. As $\mathbf{P}_F^{\ell,k} \subseteq \mathbf{P}_E^{\ell,k}$ (if two subdomains share a face they also share a vertex) we easily get that $\tau_E \leq \tau_F$. \square

Finally, we bound $\Delta^\mathcal{E}$ and $\Delta^\mathcal{F}$ in terms of each other.

Lemma 5.6. *The following bound hold:*

$$(5.22) \quad \Delta^\mathcal{F} \lesssim (1 + \log(H/h)) |w_h|_{1/2,*}^2 + \Delta^\mathcal{E},$$

$$(5.23) \quad \Delta^\mathcal{E} \lesssim \tau_{EF} \left((1 + \log(H/h)) |w_h|_{1/2,*}^2 + \Delta^\mathcal{F} \right),$$

with τ_{EF} a constant that satisfies $\tau_{EF} \leq \tau_F$.

Proof. Let us consider the first inequality. Let F be the face common to the subdomains Ω^ℓ and Ω^k , and let E be any of the edges of F . By Lemma 5.4 we have

$$\begin{aligned} \min\{\rho_\ell, \rho_k\} |\alpha_\ell^F - \alpha_k^F|^2 &\lesssim \rho_\ell |\alpha_\ell^F - \alpha_\ell^E|^2 + \rho_k |\alpha_k^F - \alpha_k^E|^2 + \min\{\rho_\ell, \rho_k\} |\alpha_\ell^E - \alpha_k^E|^2 \lesssim \\ &\lesssim (1 + \log(H/h)) \left(\rho_\ell |w_h^\ell|_{H^{1/2}(F)}^2 + \rho_k |w_h^k|_{H^{1/2}(F)}^2 \right) + \min\{\rho_\ell, \rho_k\} |\alpha_\ell^E - \alpha_k^E|^2. \end{aligned}$$

In view of the definition of $\Delta^\mathcal{F}$ and $\Delta^\mathcal{E}$, the bound (5.22) follows up adding the contribution of all faces.

Let us now consider the second bound. Let E be an edge, and let $\ell, k \in \mathcal{N}_E$. Assume at first that Ω^ℓ and Ω^k share a face F . Then, as we did for the previous bound, it is not difficult to prove that

$$\min\{\rho_\ell, \rho_k\} |\alpha_\ell^E - \alpha_k^E|^2 \lesssim (1 + \log(H/h)) \left(\rho_\ell |w_h^\ell|_{H^{1/2}(F)}^2 + \rho_k |w_h^k|_{H^{1/2}(F)}^2 \right) + \min\{\rho_\ell, \rho_k\} |\alpha_\ell^F - \alpha_k^F|^2.$$

Let us now assume that Ω^ℓ and Ω^k do not share a face. Proceeding as in the proof of the previous lemma it is easy to see that bound (5.23) holds with

$$\tau_{EF} = \max_{(\ell,k): \Omega^\ell, \Omega^k \text{ share an edge}} \left(\min\{\rho_\ell, \rho_k\} \tau_F^{\ell,k} \right).$$

As two subdomains that share an edge also share a vertex, we have that $\tau_{EF} \leq \tau_F$. \square

Now we have all the ingredient to prove Theorem 4.7. From 5.1 we get that to bound the condition number, we only need to bound $s(\mathcal{E}_D w_h, \mathcal{E}_D w_h)$ in terms of $s(w_h, w_h)$. By using Lemma 5.20, 5.21, 5.22 and 5.23 we can easily obtain that:

$$(5.24) \quad \text{if } \widetilde{W}_h \subseteq \widetilde{W}_h^E \quad |\mathcal{E}_D w_h|^2 \lesssim ((1 + \log(H/h)) + \tau_E)(1 + \log(H/h))|w_h|^2;$$

$$(5.25) \quad \text{if } \widetilde{W}_h \subseteq \widetilde{W}_h^F \quad |\mathcal{E}_D w_h|^2 \lesssim ((1 + \log(H/h)) + \tau_F)(1 + \log(H/h))|w_h|^2;$$

$$(5.26) \quad \text{if } \widetilde{W}_h \subseteq \widetilde{W}_h^V \cap \widetilde{W}_h^E \quad |\mathcal{E}_D w_h|^2 \lesssim (1 + \log(H/h))^2 |w_h|^2;$$

$$(5.27) \quad \text{if } \widetilde{W}_h \subseteq \widetilde{W}_h^V \cap \widetilde{W}_h^F \quad |\mathcal{E}_D w_h|^2 \lesssim ((1 + \log(H/h)) + \tau_{EF})(1 + \log(H/h))|w_h|^2.$$

Remark 5.7. Observe that, since we are in the framework of [35], we have the equivalence of the BDDC preconditioner with the FETI-DP preconditioner. Therefore the analysis presented also yields an estimate on the BDDC preconditioner for the Virtual Element Method.

6. NUMERICAL TESTS

We consider the model problem

$$(6.1a) \quad -\nabla \cdot (\rho \nabla u) = f \quad \text{in } \Omega = (0, 1)^3,$$

$$(6.1b) \quad u = 0 \quad \text{on } \partial\Omega.$$

We deal with meshes made of either truncated octahedra or Voronoi cells (see Figure 1); Table 1 lists the values of the following geometrical parameters for the reference meshes used in the experiments:

- $h = \max_{K \in \mathcal{T}_h} h_K$, where h_K is the diameter of element $K \in \Omega_h$.
- $h_{\min} = \min_{K \in \mathcal{T}_h} h_{\min, K}$, where $h_{\min, K}$ is the minimum distance between any two vertices of K .
- $\gamma_\star = \min_{K \in \mathcal{T}_h} \gamma_K$, where γ_K is the parameter given in Definition 2.1.

From Table 1 we see that Voronoi meshes satisfy Assumption 2.2 but with worse constants than the octahedra ones.

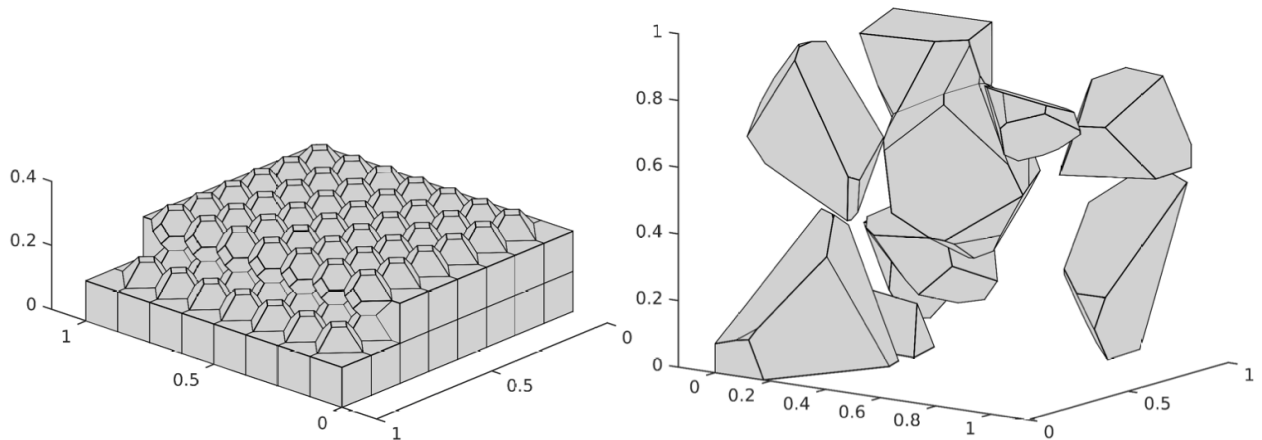


FIGURE 1. (Left): clipped view of a mesh made of truncated octahedra; (right) example cells of a Voronoi mesh.

Problem (6.1) is discretized with virtual elements of degree 1. In all experiments Ω is divided into $L = N \times N \times N$ cubic subdomains with side length $H = 1/N$. For simplicity, subdomain meshes

Mesh	h	h_{\min}	γ_*	Mesh	h	h_{\min}	γ_*
oct ₁	$4.33 \cdot 10^{-1}$	$6.25 \cdot 10^{-2}$	$6.06 \cdot 10^{-2}$	voro ₁	$7.16 \cdot 10^{-1}$	$2.40 \cdot 10^{-4}$	$9.08 \cdot 10^{-7}$
oct ₂	$2.89 \cdot 10^{-1}$	$4.17 \cdot 10^{-2}$	$6.06 \cdot 10^{-2}$	voro ₂	$5.66 \cdot 10^{-1}$	$2.48 \cdot 10^{-4}$	$4.83 \cdot 10^{-7}$
oct ₃	$2.17 \cdot 10^{-1}$	$3.13 \cdot 10^{-2}$	$6.06 \cdot 10^{-2}$	voro ₃	$5.37 \cdot 10^{-1}$	$1.26 \cdot 10^{-4}$	$3.48 \cdot 10^{-8}$
oct ₄	$1.73 \cdot 10^{-1}$	$2.50 \cdot 10^{-2}$	$6.06 \cdot 10^{-2}$	voro ₄	$3.62 \cdot 10^{-1}$	$2.60 \cdot 10^{-5}$	$6.77 \cdot 10^{-9}$
oct ₅	$1.44 \cdot 10^{-1}$	$2.08 \cdot 10^{-2}$	$6.06 \cdot 10^{-2}$	voro ₅	$2.81 \cdot 10^{-1}$	$5.69 \cdot 10^{-6}$	$1.92 \cdot 10^{-8}$
oct ₆	$1.24 \cdot 10^{-1}$	$1.79 \cdot 10^{-2}$	$6.06 \cdot 10^{-2}$	voro ₆	$2.46 \cdot 10^{-1}$	$3.12 \cdot 10^{-6}$	$3.38 \cdot 10^{-9}$
oct ₇	$1.08 \cdot 10^{-1}$	$1.56 \cdot 10^{-2}$	$6.06 \cdot 10^{-2}$	voro ₇	$1.90 \cdot 10^{-1}$	$1.31 \cdot 10^{-6}$	$7.24 \cdot 10^{-11}$
oct ₈	$9.62 \cdot 10^{-2}$	$1.39 \cdot 10^{-2}$	$6.06 \cdot 10^{-2}$	voro ₈	$1.48 \cdot 10^{-1}$	$5.93 \cdot 10^{-8}$	$5.32 \cdot 10^{-12}$

TABLE 1. Data for the meshes used in the experiments: (left) meshes made of truncated octahedra; (right) meshes made of Voronoi cells.

are obtained by rescaling and reflecting one of the meshes of the unit cube shown in Figure 1 and Table 1.

Concerning the space \widetilde{W}_h , the following choices from Section 5 are tested:

E: $\widetilde{W}_h = \widetilde{W}_h^E$;

F: $\widetilde{W}_h = \widetilde{W}_h^F$;

VE: $\widetilde{W}_h = \widetilde{W}_h^V \cap \widetilde{W}_h^E$;

VF: $\widetilde{W}_h = \widetilde{W}_h^V \cap \widetilde{W}_h^F$;

For the sake of completeness, we also test

V: $\widetilde{W}_h = \widetilde{W}_h^V$,

for which we expect a worse behaviour, as for the finite element case, where the condition number increases as $(1 + \log(H/h))^2(H/h)$ (see [45], Remark 6.39).

Edge and face constraints are imposed using an explicit change of basis. To simplify the implementation, we work with a fully redundant set of Lagrange multipliers for the dual part of the solution.

In order to analyze the performance of these algorithms, we carry out two series of experiments:

Test 1: FETI-DP scalability. We fix the subdomain problem size by choosing a reference mesh (either oct₃ or voro₅ in Table 1) and increase the number of subdomains and thus the overall problem size, but keeping H/h fixed. Table 2 shows the dimension of the primal spaces \widetilde{W}_h for the different algorithms. According to Theorem 4.7, we expect the condition number for the FETI-DP preconditioner to remain constant asymptotically.

Test 2: FETI-DP quasi-optimality. We fix the number of subdomains L to 216 ($6 \times 6 \times 6$), so that H is kept constant, and increase the size of the local problems by choosing finer and finer reference meshes (from oct₁ to oct₈, or from voro₁ to voro₈ in Table 1), thereby incrementing the overall problem size. This results in a smaller h and a bigger H/h .

According to Theorem 4.7, we now expect the condition number for the FETI-DP preconditioner to exhibit a polylogarithmic behavior asymptotically.

To test the robustness of FETI-DP, each test is run with two types of data

- constant coefficients $\rho_{|\Omega_\ell} = 1 \quad \forall \ell, f = \sin(2\pi x) \sin(2\pi y) \sin(2\pi z)$;

- coefficient jumps of 10^{10} in a 3D checkerboard distribution ($\rho_1 = 10^5, \rho_2 = 10^{-5}$). The right hand side f is implicitly chosen by choosing a right hand side vector with values uniformly randomly distributed in $[-1, 1]$.

We use the conjugate gradient with the FETI-DP Dirichlet preconditioner, with zero initial guess and, as a stopping criterion, the relative reduction of the dual residual by either 10^{-6} or 10^{-12} when using the first or the second type of data, respectively. MATLAB[®] R2016b is used as the subdomain and coarse sparse direct solver. All the experiments are run on a machine equipped with processor Intel[®] Core™ i7-7820HQ, operating system Ubuntu Linux 16.04 LTS, memory 64GB, 2400MHz DDR4 Non-ECC SDRAM.

L	Octahedra		Voronoi		Coarse				
	h	D.o.f.	h	D.o.f.	V	E	F	VE	VF
8	$1.08 \cdot 10^{-1}$	31 928	$1.40 \cdot 10^{-1}$	46 416	1	6	12	7	13
64	$5.41 \cdot 10^{-2}$	261 960	$7.02 \cdot 10^{-2}$	388 280	27	108	144	135	171
216	$3.61 \cdot 10^{-2}$	892 072	$4.68 \cdot 10^{-2}$	1 330 240	125	450	540	575	665
512	$2.71 \cdot 10^{-2}$	2 124 248	$3.51 \cdot 10^{-2}$	3 176 952	343	1176	1344	1519	1687
1000	$2.17 \cdot 10^{-2}$	4 160 472	$2.81 \cdot 10^{-2}$	6 233 072	729	2430	2700	3159	3429
1728	$1.80 \cdot 10^{-2}$	7 202 728	$2.34 \cdot 10^{-2}$	10 803 256	1331	4356	4752	5687	6083

TABLE 2. Number of global and primal d.o.f. for the different algorithms considered and the meshes of Test 1: constant H/h , reference subdomain mesh oct_3 (octahedra) or vor_5 (Voronoi).

L	V		E		F		VE		VF	
	κ	it	κ	it	κ	it	κ	it	κ	it
8	1.00	1	1.00	1	1.00	1	1.00	1	1.00	1
64	3.23	9	2.39	8	2.33	8	1.58	7	2.15	8
216	12.85	12	2.67	10	2.95	10	1.58	7	2.64	10
512	13.75	18	2.59	10	3.05	11	1.61	7	2.57	10
1000	13.92	18	2.53	10	3.27	11	1.62	7	2.70	10
1728	13.98	18	2.51	10	3.38	11	1.63	7	2.75	10

TABLE 3. Test 1 - truncated octahedra meshes, $H/h = 4.6188$ and constant coefficients $\rho = 1$. Condition number estimates and iteration numbers for the different choices of \widetilde{W}_h .

6.1. FETI-DP scalability. Results for the first series of experiments (Test 1) with constant coefficients ρ are reported in Table 3 for meshes of truncated octahedra, and in Table 4 for Voronoi meshes. The results are in accordance with the theoretical bounds for both set of meshes, confirming the robustness of the preconditioner. Tables 3 and 4 show that, without any jumps in the coefficients, the results for E, F, VE and VE are similar. In switching from the octahedra to the Voronoi mesh, which satisfies Assumption 2.2 but with worse constants, we observe an increase in the number of iterations and in the condition number which, however, still display the expected behavior. As one expects, the choice V is instead not competitive.

L	V		E		F		VE		VF	
	κ	it	κ	it	κ	it	κ	it	κ	it
8	1.00	1	1.00	1	1.00	1	1.00	1	1.00	1
64	27.88	19	4.72	15	6.36	15	3.92	13	5.51	14
216	26.53	25	6.03	17	9.45	19	4.16	14	7.79	17
512	29.05	31	6.09	17	10.54	21	4.16	14	8.38	18
1000	29.55	32	6.14	17	11.03	21	4.16	14	8.73	19
1728	30.47	32	6.17	17	11.43	22	4.16	14	8.89	19

TABLE 4. Test 1 - Voronoi meshes, $H/h = 6.171687$ and constant coefficients $\rho = 1$. Condition number estimates and iteration numbers for the different choices of \widetilde{W}_h .

The numerical tests with varying coefficients ρ are displayed in Table 5 and Table 6 for octahedra and Voronoi meshes respectively. With highly oscillating coefficients, the choice F of \widetilde{W}_h , i.e when only continuity of face averages across subdomains is imposed, performs very poorly on both types of meshes, despite their different degree of regularity. We note that, with jumping coefficients, the bound given in Theorem 4.7 for E, F or VF would become meaningless if τ_E, τ_F or τ_{EF} are high enough.

L	V		E		F		VE		VF	
	κ	it	κ	it	κ	it	κ	it	κ	it
8	1.87	6	1.75	5	2.73	6	1.25	5	2.17	6
64	10.33	13	2.57	8	$4.48 \cdot 10^9$	31	1.28	5	11.69	11
216	10.36	15	2.53	8	$5.59 \cdot 10^9$	88	1.28	5	12.62	15
512	10.35	15	2.54	8	$6.06 \cdot 10^9$	118	1.29	5	13.37	16
1000	10.36	15	2.54	8	$6.29 \cdot 10^9$	132	1.29	5	13.28	16
1728	10.37	15	2.54	8	$6.44 \cdot 10^9$	138	1.29	5	13.17	16

TABLE 5. Test 1 - truncated octahedra meshes, H/h constant, checkerboard ($\rho_1 = 10^5, \rho_2 = 10^{-5}$), f uniform random in $[-1, 1]$. Condition number estimates and iteration numbers for the different choices of \widetilde{W}_h .

L	V		E		F		VE		VF	
	κ	it	κ	it	κ	it	κ	it	κ	it
8	4.95	11	3.60	9	6.74	11	3.20	8	5.71	11
64	23.73	20	6.58	13	$1.14 \cdot 10^{10}$	71	3.55	9	32.30	19
216	25.53	26	6.69	13	$1.45 \cdot 10^{10}$	175	3.58	9	35.94	27
512	25.73	27	6.70	13	$1.57 \cdot 10^{10}$	228	3.58	9	36.97	28
1000	25.87	27	6.68	13	$1.65 \cdot 10^{10}$	254	3.57	9	37.81	29
1728	25.91	27	6.69	13	$1.69 \cdot 10^{10}$	269	3.58	9	38.11	29

TABLE 6. Test 1 - Voronoi meshes, H/h constant, checkerboard ($\rho_1 = 10^5, \rho_2 = 10^{-5}$), f uniform random in $[-1, 1]$. Condition number estimates and iteration numbers for the different choices of \widetilde{W}_h .

Indeed, with coefficient jumps of 10^{10} in a checkerboard distribution, we have $\tau_E = 1, \tau_F = 10^{10}$, and $\tau_{EF} = 10^{10}$, in agreement with the better performance of E with respect to F and VF, as shown in Tables 5, 6. The independence from the jumps of the coefficients is shown by VE as predicted by the bound of Theorem 4.7.

6.2. FETI-DP quasi-optimality. Results for our second set of runs (Test 2) with both smooth and random data are shown in Figures 2 and 3 for meshes of truncated octahedra, and in Figures 4 and 5 for Voronoi meshes. Both sets of runs are in agreement with the condition number estimates of Theorem 4.7. In particular, the experiments show that FETI-DP achieves good scalability for our model problem if VE is used, i.e. $\widetilde{W}_h \subset \widetilde{W}_h^V \cap \widetilde{W}_h^E$.

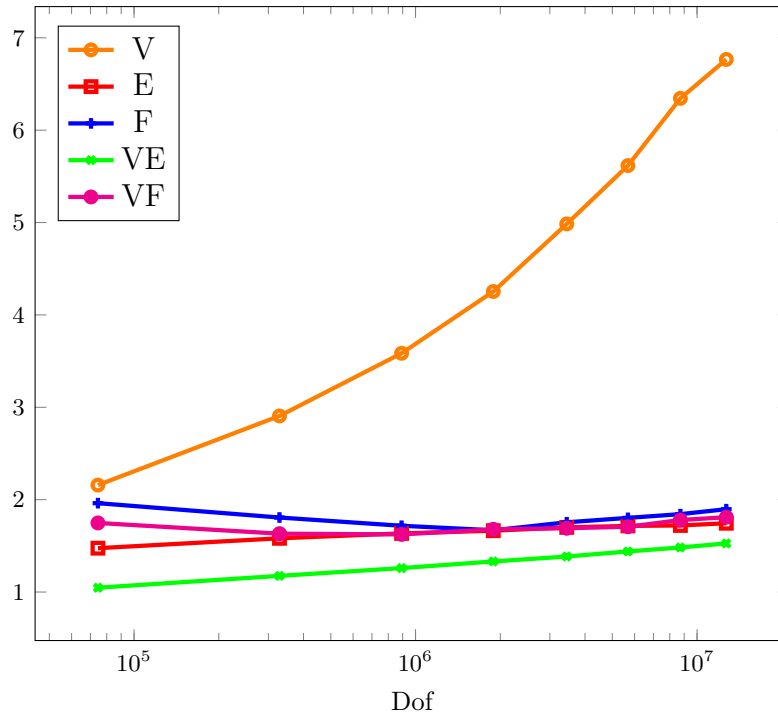


FIGURE 2. Test 2 - constant coefficients $\rho = 1$, truncated octahedra meshes. Plots of $\kappa^{1/2}$ as a function of the global degrees of freedom on meshes of Voronoi meshes for the different choices of \widetilde{W}_h .

REFERENCES

1. P. F. Antonietti, A. Cangiani, J. Collis, Z. Dong, E. H. Georgoulis, S. Giani, and P. Houston, *Review of discontinuous Galerkin finite element methods for partial differential equations on complicated domains*, Connections and Challenges in Modern Approaches to Numerical Partial Differential Equations, Springer, 2016, pp. 279–308.
2. P. F. Antonietti, L. Beirão da Veiga, D. Mora, and M. Verani, *A stream virtual element formulation of the Stokes problem on polygonal meshes*, SIAM Journal on Numerical Analysis **52** (2014), no. 1, 386–404.
3. P. F. Antonietti, L. Beirão da Veiga, S. Scacchi, and M. Verani, *A C^1 virtual element method for the Cahn-Hilliard equation with polygonal meshes*, SIAM Journal on Numerical Analysis **54** (2016), no. 1, 34–56.
4. P. F. Antonietti, L. Mascotto, and M. Verani, *A multigrid algorithm for the p -version of the virtual element method*, Math. Model. Numer. Anal. **52** (2018), no. 1, 337–364.
5. L. Beirão da Veiga, F. Brezzi, A. Cangiani, G. Manzini, L. D. Marini, and A. Russo, *Basic principles of virtual element methods*, Mathematical Models and Methods in Applied Sciences **23** (2013), no. 1, 199–214.

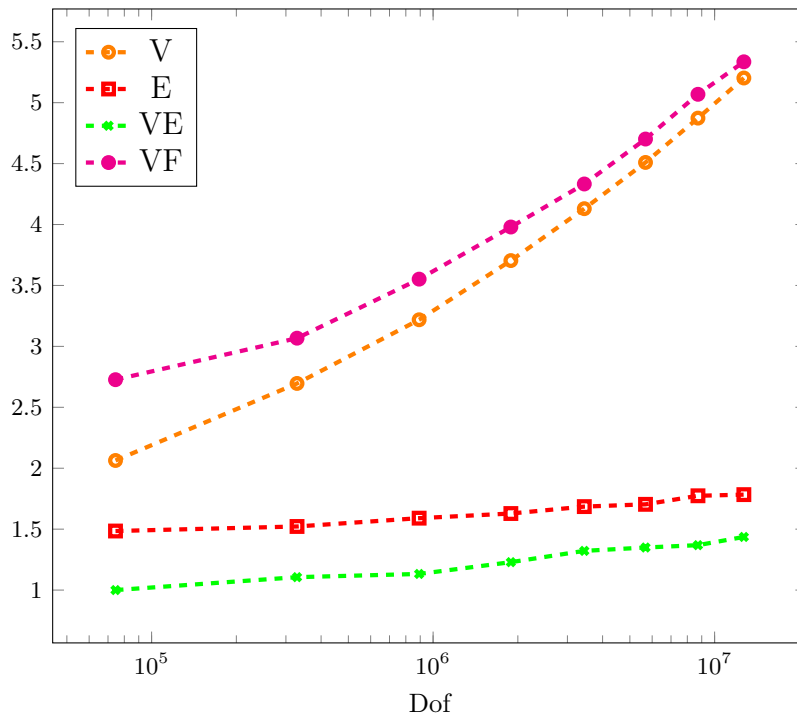


FIGURE 3. Test 2 - varying coefficients, checkerboard ($\rho_1 = 10^5, \rho_2 = 10^{-5}$), f uniform random in $[-1, 1]$, truncated octahedra meshes. Plots of $\kappa^{1/2}$ as a function of the global degrees of freedom for the different choices of \widetilde{W}_h , except \widetilde{W}_h^F .

6. L. Beirão da Veiga, F. Brezzi, and L. Marini, *Virtual elements for linear elasticity problems*, SIAM Journal on Numerical Analysis **51** (2013), no. 2, 794–812.
7. L. Beirão da Veiga, F. Brezzi, L. D. Marini, and A. Russo, *The Hitchhiker’s guide to the virtual element method*, Mathematical Models and Methods in Applied Sciences **24** (2014), no. 8, 1541–1573.
8. ———, *Mixed virtual element methods for general second order elliptic problems on polygonal meshes*, ESAIM: M2AN **50** (2016), no. 3, 727–747.
9. ———, *Virtual Element Method for general second-order elliptic problems on polygonal meshes*, Mathematical Models and Methods in Applied Sciences **26** (2016), no. 4, 729–750.
10. L. Beirão da Veiga, A. Chernov, L. Mascotto, and A. Russo, *Basic principles of hp virtual elements on quasiuniform meshes*, Mathematical Models and Methods in Applied Sciences **26** (2016), no. 8, 1567–1598.
11. L. Beirão da Veiga, K. Lipnikov, and G. Manzini, *The mimetic finite difference method for elliptic problems*, MS&A, no. 11, Springer, 2014.
12. L. Beirão da Veiga, C. Lovadina, and G. Vacca, *Divergence free virtual elements for the Stokes problem on polygonal meshes*, ESAIM: M2AN **51** (2017), no. 2, 509–535.
13. ———, *Virtual Elements for the Navier-Stokes problem on polygonal meshes*, arXiv e-prints (2017).
14. M. F. Benedetto, S. Berrone, and S. Scialó, *A globally conforming method for solving flow in discrete fracture networks using the virtual element method*, Finite Elements in Analysis and Design **109** (2016), 23 – 36.
15. S. Berrone and A. Borio, *Orthogonal polynomials in badly shaped polygonal elements for the Virtual Element Method*, Finite Elements in Analysis and Design **129** (2017), 14–31.
16. S. Bertoluzza, M. Pennacchio, and D. Prada, *BDDC and FETI-DP for the virtual element method*, Calcolo **54** (2017), 1565–1593.
17. J. H. Bramble, J. E. Pasciak, and A. H. Schatz, *The construction of preconditioners for elliptic problems by substructuring, IV*, Math. Comp. **53** (1989), 1–24.
18. S. C. Brenner and L. Y. Sung, *BDDC and FETI-DP without matrices or vectors*, Computer Methods in Applied Mechanics and Engineering **196** (2007), no. 8, 1429 – 1435.
19. F. Brezzi, K. Lipnikov, and M. Shashkov, *Convergence of mimetic finite difference methods for diffusion problems on polyhedral meshes*, SIAM Journal on Numerical Analysis **43** (2005), 1872–1896.

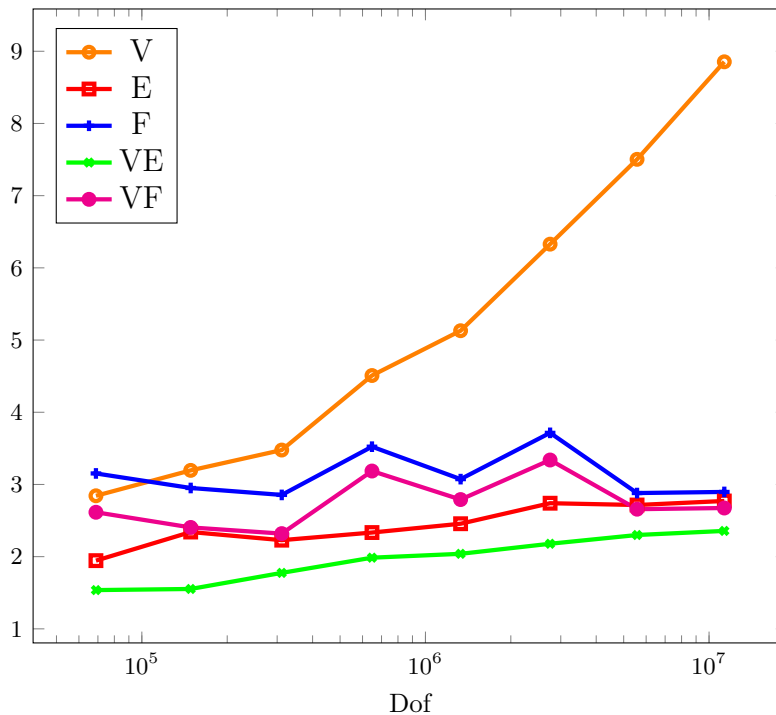


FIGURE 4. Test 2 - constant coefficients $\rho = 1$, Voronoi meshes. Plots of $\kappa^{1/2}$ as a function of the global degrees of freedom on meshes of Voronoi meshes for the different choices of \widetilde{W}_h .

20. J.G. Calvo, *On the approximation of a virtual coarse space for domain decomposition methods in two dimensions*, Math. Models Methods Appl. Sci. **38** (2018), no. 7, 1267–1289.
21. ———, *An overlapping schwarz method for virtual element discretizations in two dimensions*, (available, november 2018).
22. A. Cangiani, E. H. Georgoulis, and P. Houston, *hp-version discontinuous Galerkin methods on polygonal and polyhedral meshes*, Mathematical Models and Methods in Applied Sciences **24** (2014), no. 10, 2009–2041.
23. A. Cangiani, E.H. Georgoulis, T. Pryer, and O.J. Sutton, *A posteriori error estimates for the virtual element method*, Numer. Math. (2017), 857–893.
24. B. Cockburn, B. Dong, and J. Guzmán, *A superconvergent LDG-hybridizable Galerkin method for second-order elliptic problems*, Mathematics of Computation **77** (2008), no. 264, 1887–1916.
25. L. Beirão da Veiga, C. Lovadina, and D. Mora, *A virtual element method for elastic and inelastic problems on polytope meshes*, Computer Methods in Applied Mechanics and Engineering **295** (2015), 327 – 346.
26. D. A. Di Pietro and A. Ern, *Hybrid high-order methods for variable-diffusion problems on general meshes*, Comptes Rendus Mathématique **353** (2015), no. 1, 31–34.
27. C. Farhat, M. Lesoinne, P. LeTallec, K. Pierson, and D. Rixen, *FETI-DP: A Dual-Primal unified FETI method - Part I: A faster alternative to the two-level FETI method*, International Journal for Numerical Methods in Engineering **50** (2001), 1523–1544.
28. M. Frittelli and I. Sgura, *Virtual Element Method for the Laplace-Beltrami equation on surfaces*, arXiv e-prints (2016).
29. A. L. Gain, C. Talischi, and G. H. Paulino, *On the virtual element method for three-dimensional linear elasticity problems on arbitrary polyhedral meshes*, Computer Methods in Applied Mechanics and Engineering **282** (2014), 132–160.
30. H. H. Kim, *A FETI-DP formulation of three dimensional elasticity problems with mortar discretization*, SIAM Journal on Numerical Analysis **46** (2008), no. 5, 2346–2370.
31. A. Klawonn, L. F. Pavarino, and O. Rheinbach, *Spectral element FETI-DP and BDDC preconditioners with multi-element subdomains*, Computer Methods in Applied Mechanics and Engineering **198** (2008), no. 3, 511–523.

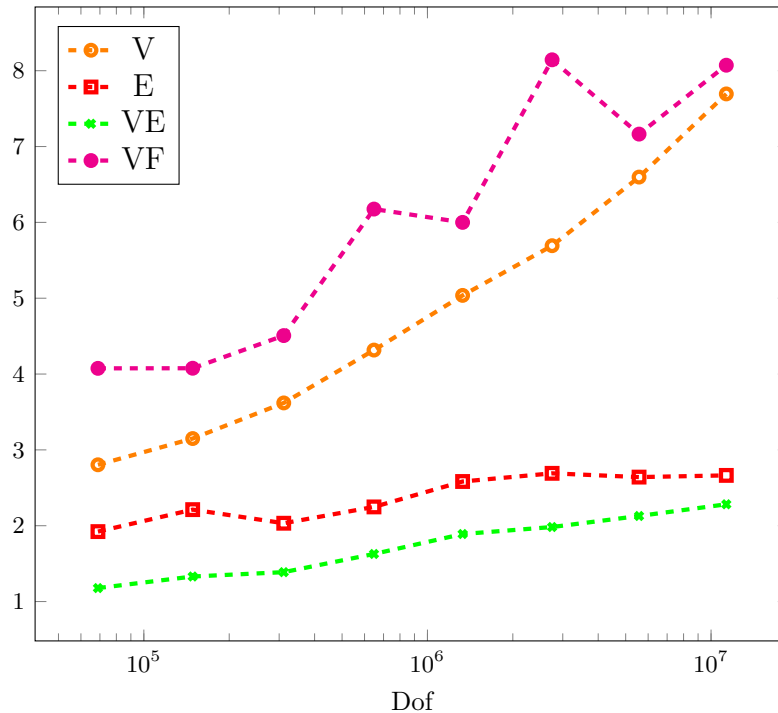


FIGURE 5. Test 2 - varying coefficients, checkerboard ($\rho_1 = 10^5, \rho_2 = 10^{-5}$), f uniform random in $[-1, 1]$, Voronoi meshes. Plots of $\kappa^{1/2}$ as a function of the global degrees of freedom for the different choices of \widetilde{W}_h , except \widetilde{W}_h^F .

32. A. Klawonn and O. B. Widlund, *Dual-primal FETI methods for linear elasticity*, Communications on Pure and Applied Mathematics **59** (2006), no. 11, 1523–1572.
33. K. Lipnikov, *On shape-regularity of polyhedral meshes for solving pdes*.
34. J. Mandel, C. R. Dohrmann, and R. Tezaur, *An algebraic theory for primal and dual substructuring methods by constraints*, Applied Numerical Mathematics **54** (2005), no. 2, 167 – 193.
35. J. Mandel and B. Sousedík, *BDDC and FETI-DP under minimalist assumptions*, Computing **81** (2007), no. 4, 269–280.
36. L. Mascotto, *Ill-conditioning in the virtual element method: Stabilizations and bases*, Numerical Methods for Partial Differential Equations **34** (2018), no. 4, 1258–1281.
37. L. Mascotto, L. Beirão da Veiga, A. Chernov, and A. Russo, *Exponential convergence of the hp Virtual Element Method with corner singularities*, Numer. Math. (2018), 138–581.
38. L. F. Pavarino, *BDDC and FETI-DP preconditioners for spectral element discretizations*, Computer Methods in Applied Mechanics and Engineering **196** (2007), no. 8, 1380–1388.
39. L. F. Pavarino and S. Scacchi, *Isogeometric block feti-dp preconditioners for the stokes and mixed linear elasticity systems*, Computer Methods in Applied Mechanics and Engineering **310** (2016), 694–710.
40. I. Perugia, P. Pietra, and A. Russo, *A plane wave virtual element method for the Helmholtz problem*, ESAIM: M2AN **50** (2016), no. 3, 783–808.
41. D. Prada, S. Bertoluzza, M. Pennacchio, and M. Livesu, *FETI-DP preconditioners for the Virtual Element Method on general 2D meshes*, in Numerical Mathematics and Advanced Applications - ENUMATH 2017, Springer International Publishing, to appear.
42. D. S. Rjasanow and S. Weißer, *Higher order BEM-based FEM on polygonal meshes*, SIAM Journal on Numerical Analysis **241** (2013), 103–115.
43. B. F. Smith, *A domain decomposition algorithm for elliptic problems in three dimensions*, Numer. Math. **60** (1991), no. 2, 219–234.
44. N. Sukumar and A. Tabarraei, *Conforming polygonal finite elements*, International Journal for Numerical Methods in Engineering **61** (2004), no. 12, 2045–2066.

45. A. Toselli and O. Widlund, *Domain decomposition methods - algorithms and theory*, Springer Series in Computational Mathematics, vol. 34, Springer, 2004.
46. G. Vacca and L. Beirão da Veiga, *Virtual element methods for parabolic problems on polygonal meshes*, Numerical Methods for Partial Differential Equations **31** (2015), no. 6, 2110–2134.
47. J. Wang and X. Ye, *A weak Galerkin finite element method for second-order elliptic problems*, Journal of Computational and Applied Mathematics **241** (2013), 103–115.

IMATI “E. MAGENES”, CNR, PAVIA (ITALY)
E-mail address: `silvia.bertoluzza@imati.cnr.it`

IMATI “E. MAGENES”, CNR, PAVIA (ITALY)
E-mail address: `micol.pennacchio@imati.cnr.it`

IMATI “E. MAGENES”, CNR, PAVIA (ITALY)
E-mail address: `daniele.prada@imati.cnr.it`